

## A SECOND-ORDER ACCURATE, OPERATOR SPLITTING SCHEME FOR REACTION-DIFFUSION SYSTEMS IN AN ENERGETIC VARIATIONAL FORMULATION\*

CHUN LIU<sup>†</sup>, CHENG WANG<sup>‡</sup>, AND YIWEI WANG<sup>§</sup>

**Abstract.** A second-order accurate in time, positivity-preserving, and unconditionally energy stable operator splitting scheme is proposed and analyzed for reaction-diffusion systems with the detailed balance condition. The scheme is designed based on an energetic variational formulation, in which the reaction part is reformulated in terms of the reaction trajectory, and both the reaction and diffusion parts dissipate the same free energy. At the reaction stage, the reaction trajectory equation is approximated by a second-order Crank–Nicolson type method. The unique solvability, positivity-preserving property, and energy stability are established based on a convexity analysis. In the diffusion stage, an exact integrator is applied if the diffusion coefficients are constant, and a Crank–Nicolson type scheme is constructed if the diffusion part is nonlinear. In either case, both the positivity-preserving property and energy stability could be theoretically established. Moreover, a combination of the numerical algorithms at both stages by the Strang splitting approach leads to a second-order accurate, structure-preserving scheme for the original reaction-diffusion system. Numerical experiments are presented, which demonstrate the accuracy and the energy stability of the proposed scheme.

**Key words.** reaction-diffusion system, energetic variational formulation, operator splitting scheme, positivity-preserving, energy stability, second-order

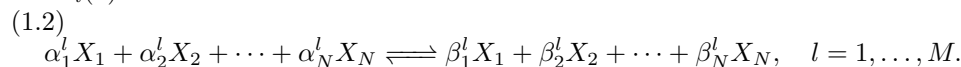
**MSC codes.** 35K35, 35K55, 49J40, 65M06, 65M12

**DOI.** 10.1137/21M1444825

**1. Introduction.** In this work, we consider the reaction-diffusion system

$$(1.1) \quad \partial_t c_i = \nabla \cdot (D_i(c_i, \mathbf{x}) \nabla c_i) + r_i(\mathbf{c}), \quad i = 1, \dots, N,$$

where  $c_i > 0$  is the concentration of  $i$ th species,  $D_i(c_i, \mathbf{x})$  are diffusion coefficients, and  $r_i(\mathbf{c})$  are nonlinear reaction terms for the chemical reactions



Reaction-diffusion systems of this type can be found in many mathematical models in chemical engineering, biology, soft matter physics, and combustion theory; see [11, 32, 33, 37, 41, 50, 56, 57, 58, 63, 65] for examples.

Numerical simulation for the reaction-diffusion system (1.1) is often challenging, due to the nonlinearity and stiffness brought by the reaction term. Moreover, a naive discretization to (1.1) may fail to preserve the positivity of  $c_i$  and the conservation

---

\*Submitted to the journal's Methods and Algorithms for Scientific Computing section September 7, 2021; accepted for publication (in revised form) March 28, 2022; published electronically August 2, 2022.

<https://doi.org/10.1137/21M1444825>

**Funding:** The first and third authors were partially supported by National Science Foundation grants DMS-1759536 and DMS-1950868. The second author was partially supported by National Science Foundation grant DMS-2012669.

<sup>†</sup>Department of Applied Mathematics, Illinois Institute of Technology, Chicago, IL 60616 USA (cliu124@iit.edu).

<sup>‡</sup>Department of Mathematics, University of Massachusetts, North Dartmouth, MA 02747 USA (cwang1@umassd.edu).

<sup>§</sup>Corresponding author. Department of Applied Mathematics, Illinois Institute of Technology, Chicago, IL 60616 USA (ywang487@iit.edu).

property in the original system [25]. To overcome these difficulties, many numerical schemes have been developed to solve reaction kinetics and reaction-diffusion systems [6, 25, 36, 67], including some operator splitting approaches [9, 16, 28, 29, 67].

It has been discovered that if the reaction term in (1.1) satisfies the law of mass action with the detailed balance condition, the whole system admits an energy-dissipation law, which opens a door to develop structure-preserving numerical schemes for such a system. In more detail, under certain conditions, which will be specified in the next section, the reaction-diffusion system (1.1) can be reformulated as a combination of a gradient flow of the reaction trajectory  $\mathbf{R}(\mathbf{x}, t)$  and a gradient flow of species concentration  $\mathbf{c}(\mathbf{x}, t)$  for a single free energy [64]. Since the reaction and diffusion parts dissipate the same free energy, it is natural to use an operator splitting approach to develop an energy stable scheme for the whole system. Based on this variational structure, a first-order accurate operator splitting scheme has been constructed in a recent work [45], with the variational structure theoretically preserved for the numerical solution. In this approach, since the physical free energy is in the form of logarithmic functions of the concentration  $\mathbf{c}(\mathbf{x})$ , which is a linear function of reaction trajectories  $\mathbf{R}(\mathbf{x})$ , the positivity-preserving analysis of the numerical scheme at both stages has been established. Similar to the analysis in a recent article [10] for the Flory–Huggins Cahn–Hilliard flow, an implicit treatment of the nonlinear singular logarithmic term is crucial to theoretically justify its positivity-preserving property. A more careful analysis reveals that the convex and the singular natures of the implicit nonlinear parts prevent the numerical solutions from approaching the singular limiting values, so that the positivity-preserving property is available for the density variables of all the species. A detailed convergence analysis and error estimate have also been reported in a recent work [46]. However, it is a not trivial task to develop a second-order accurate operator splitting scheme based on this idea, since most existing second-order energy stable schemes for gradient flows are multistep algorithms based on either modified Crank–Nicolson or BDF2 temporal discretization. Moreover, to ensure both the unique solvability and energy stability, a multistep approximation to the concave terms is usually needed. Furthermore, a single-step, second-order approximation has to be accomplished at each stage in the operator splitting approach, and a theoretical justification of the positivity-preserving property and energy stability is also very challenging.

The purpose of this paper is to propose and analyze a second-order accurate operator splitting scheme for the reaction-diffusion system with the detailed balance condition. Following the energetic variational formulation, the splitting scheme solves the reaction trajectory equation of  $\mathbf{R}$  at the reaction stage, and solves the diffusion equation for  $\mathbf{c}$  in the diffusion stage. To overcome the above-mentioned difficulties, we make use of a numerical profile created by the first-order convex splitting algorithm, which is proved to be a second-order accurate approximation to the physical quantity at time step  $t^{n+1}$ , to construct a second-order approximation to the mobility part. Then an application of a modified Crank–Nicolson formula leads to a second-order approximation to the mobility function at the intermediate time instant  $t^{n+1/2}$ . Meanwhile, the physical energy does not contain any concave part in the reaction-diffusion system, so that a single-step, modified Crank–Nicolson method leads to a second-order accurate algorithm. In addition, an artificial second-order Douglas–Dupont type regularization term [10], in the form of  $\Delta t \sum_{i=1}^N \sigma_i(\mu_i(R^{n+1}) - \mu_i(R^n))$ , is added to ensure the positivity-preserving property. The energy stability is derived by a careful energy estimate because of the choice in the modified Crank–Nicolson approximation. These techniques lead to a second-order accurate, positivity-preserving, and energy stable

algorithm in the reaction stage.

In the diffusion stage, an exact integrator, the so-called exponential time differencing (ETD) method, is applied if the diffusion coefficients are constant. Such an ETD method solves the diffusion stage equation exactly (by keeping the finite difference spatial discretization), so that both the positivity-preserving property and energy stability are ensured. If the diffusion coefficients are nonlinear, we have to follow an idea from the reaction stage and apply a predictor-corrector approach in the mobility approximation and a modified Crank–Nicolson algorithm for the chemical potential. In either case, both the positivity-preserving property and energy stability could be theoretically justified for the numerical solution in the diffusion stage. Finally, a combination of the numerical algorithms at both stages by the Strang splitting approach leads to a second-order accurate, structure-preserving scheme for the original reaction-diffusion system.

The rest of this paper is organized as follows. The energetic variational approach for the reaction-diffusion systems with the detailed balance condition is reviewed in section 2. Subsequently, the second-order operator splitting scheme is presented in section 3. The positivity-preserving and energy stability analyses will be provided at each stage as well. Some numerical results will be presented in section 4 to demonstrate the performance of the second-order operator splitting scheme.

**2. Preliminary.** In this section, we briefly review the energetic variational formulation for reaction-diffusion systems with detailed balance, which will be the foundation of the second-order operator splitting schemes developed in section 3. We refer the interested reader to [45, 64] for more detailed descriptions.

**2.1. EnVarA for diffusions.** Inspired by the seminal works of Rayleigh [60] and Onsager [52, 53], the energetic variational approach (EnVarA) [24, 30, 44] derives the dynamics of a complicated system from a prescribed energy-dissipation law. In more detail, an energy-dissipation law, which comes from the first and second laws of thermodynamics [30], can be written as

$$\frac{d}{dt}E^{\text{total}} = -\Delta,$$

for an isothermal closed system, where  $E^{\text{total}}$  is the total energy, including both the kinetic energy  $\mathcal{K}$  and the Helmholtz free energy  $\mathcal{F}$ , and  $\Delta \geq 0$  is the rate of energy dissipation which is equal to the entropy production in this case. Starting with an energy-dissipation law, the EnVarA derives the dynamics of the systems through two variational principles, the least action principle (LAP) and the maximum dissipation principle (MDP). The LAP, which states the equation of motion for a Hamiltonian system, can be derived from the variation of the action functional  $\mathcal{A} = \int_0^T \mathcal{K} - \mathcal{F} dt$ , with respect to the flow maps, and gives a unique procedure for deriving the conservative force in the system. The dissipation force in the system can be derived by the MDP, i.e., taking the variation of the dissipation potential  $\mathcal{D}$ , which equals  $\frac{1}{2}\Delta$  in the linear response regime, with respect to the rate (such as velocity). In turn, the force balance condition leads to the evolution equation of the system

$$(2.1) \quad \frac{\delta \mathcal{D}}{\delta \mathbf{x}_t} = \frac{\delta \mathcal{A}}{\delta \mathbf{x}}.$$

The energetic variational approach has been successfully applied to build up many mathematical models [30], including systems with chemical reactions [64, 65]; it has

also provided a guideline for designing structure-preserving numerical schemes for systems with variational structures [45, 48, 49].

The classical EnVarA formulation is a variational principle for continuum mechanics, and the variable  $\mathbf{x}$  in (2.1) should be understood as the flow map  $\mathbf{x}(\mathbf{X}, t)$  from a reference domain  $\Omega_0$  to a physical domain  $\Omega$  at time  $t$ . Here  $\mathbf{X} \in \Omega_0$  is the Lagrangian coordinate, and  $\mathbf{x} \in \Omega$  is the Eulerian coordinate. An important feature of a continuum mechanical system is that the evolution of physical variables, such as density, is determined by the evolution of the flow map  $\mathbf{x}(\mathbf{X}, t)$  through a kinematic relation. To define the kinematic relation, it is convenient to introduce the deformation tensor associated with the flow map  $\mathbf{x}(\mathbf{X}, t)$  by

$$\tilde{\mathbf{F}}(\mathbf{x}(\mathbf{X}, t), t) = \mathbf{F}(\mathbf{X}, t) = \nabla_{\mathbf{X}} \mathbf{x}(\mathbf{X}, t),$$

which carries all the transport/kinematic information of the microstructures, patterns, and configurations in continuum mechanical systems. Without ambiguity, we will not distinguish  $\mathbf{F}$  and  $\tilde{\mathbf{F}}$  in the following. For a density function  $\rho(\mathbf{x}, t)$ , which satisfies the conservation of mass, the kinematics can be written as

$$(2.2) \quad \rho(\mathbf{x}, t) = \rho_0(\mathbf{X}) / \det \mathbf{F}(\mathbf{X}, t)$$

in Lagrangian coordinates. Here  $\rho_0(\mathbf{X})$  is the initial density. The kinematics (2.2) is equivalent to  $\rho_t + \nabla \cdot (\rho \mathbf{u}) = 0$  in Eulerian coordinates.

Diffusion is one of the simplest mechanical processes, in which  $\mathcal{K} = 0$ . In the framework of EnVarA, a diffusion can be described by the energy-dissipation law

$$(2.3) \quad \frac{d}{dt} \mathcal{F}[\rho] = - \int_{\Omega} \eta(\rho) |\mathbf{u}|^2 d\mathbf{x}, \quad \mathcal{F}[\rho] = \int_{\Omega} \omega(\rho) d\mathbf{x},$$

where  $\rho$  is a conserved quantity,  $\mathcal{F}[\rho]$  is the free energy,  $\omega(\rho)$  is the free energy density, and  $\eta(\rho)$  is the friction coefficient. Due to the kinematics (2.2), the free energy can be reformulated as a functional of  $\mathbf{x}(\mathbf{X}, t)$  in Lagrangian coordinates, i.e.,

$$(2.4) \quad \mathcal{F}[\mathbf{x}] = \int_{\Omega_0} \omega \left( \frac{\rho_0(\mathbf{X})}{\det \mathbf{F}} \right) \det \mathbf{F} d\mathbf{X}.$$

A direct computation leads to

$$(2.5) \quad \frac{\delta \mathcal{A}}{\delta \mathbf{x}} = -\nabla \cdot \left( \frac{\partial \omega}{\partial \rho} \rho - \omega \right) = -\rho \nabla \mu,$$

where  $\mu = \frac{\delta \mathcal{F}}{\delta \rho}$  is the chemical potential. Formally, one can obtain (2.5) by using the relation  $\delta \rho = \nabla \cdot (\rho \delta \mathbf{x})$  in the notion of the principle of virtual work [4]. For the dissipation part, since  $\mathcal{D} = \frac{1}{2} \int \eta(\rho) |\mathbf{u}|^2 d\mathbf{x}$ , it is easy to compute  $\frac{\delta \mathcal{D}}{\delta \mathbf{u}} = \eta(\rho) \mathbf{u}$ . As a consequence,

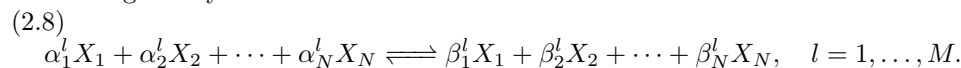
$$(2.6) \quad \eta(\rho) \mathbf{u} = -\rho \nabla \mu.$$

Combining the force balance equation (2.6) with the kinematics  $\rho_t + \nabla \cdot (\rho \mathbf{u}) = 0$ , one obtains a generalized diffusion equation

$$(2.7) \quad \rho_t = \nabla \cdot \left( \frac{\rho^2}{\eta(\rho)} \nabla \mu \right), \quad \mu = \frac{\delta \mathcal{F}}{\delta \rho}.$$

**2.2. EnVarA for reaction kinetics.** Next, we show how to extend the EnVarA framework to reaction kinetics, which is not a mechanical process determined by the flow map.

Consider a system with  $N$  species  $\{X_1, X_2, \dots, X_N\}$  and  $M$  reversible chemical reactions given by



Denote  $\mathbf{c} = (c_1, c_2, \dots, c_N)^\top$ , the concentrations of all species. The reaction kinetics of the system is often described by a system of ODEs

$$(2.9) \quad \frac{d}{dt} c_i = \sum_{l=1}^M \sigma_{il} r_l(\mathbf{c}),$$

where  $r_l(\mathbf{c})$  is the reaction rate for the  $l$ th chemical reaction, and  $\sigma_{il} = \beta_i^l - \alpha_i^l$  is the stoichiometric coefficients. From (2.9), note that

$$(2.10) \quad \frac{d}{dt} (\mathbf{e} \cdot \mathbf{c}) = \mathbf{e} \cdot \boldsymbol{\sigma} \mathbf{r}(\mathbf{c}(t), t) = 0 \quad \text{for } \mathbf{e} \in \text{Ker}(\boldsymbol{\sigma}^\top).$$

In turn, one can define  $N$ -rank  $(\boldsymbol{\sigma})$  linearly independent conserved quantities for the reaction network. In classical chemical kinetics,  $r_l(\mathbf{c})$  is determined by the law of mass action (LMA), which states that the reaction rate is directly proportional to the product of the reactant concentrations, i.e.,

$$(2.11) \quad r_l(\mathbf{c}) = k_l^+ \mathbf{c}^{\boldsymbol{\alpha}^l} - k_l^- \mathbf{c}^{\boldsymbol{\beta}^l}, \quad \mathbf{c}^{\boldsymbol{\alpha}^l} = \prod_{i=1}^N c_i^{\alpha_i^l}, \quad \mathbf{c}^{\boldsymbol{\beta}^l} = \prod_{i=1}^N c_i^{\beta_i^l},$$

in which  $k_l^+$  and  $k_l^-$  are the forward and backward reaction constants for the  $l$ th reaction.

It has been shown that the reaction kinetics (2.9), along with the LMA (2.11), admits a Lyapunov function if there exists a strictly positive equilibrium point  $\mathbf{c}_\infty \in \mathbb{R}_+^N$  satisfying

$$(2.12) \quad k_l^+ \mathbf{c}_\infty^{\boldsymbol{\alpha}^l} = k_l^- \mathbf{c}_\infty^{\boldsymbol{\beta}^l}, \quad l = 1, \dots, M.$$

Such an equilibrium point is called a *detailed balance* equilibrium. We say a reaction network satisfies the detailed balance condition if it admits a detailed balance equilibrium. Within  $\mathbf{c}_\infty$ , one can define the Lyapunov function as

$$(2.13) \quad \mathcal{F}[\mathbf{c}] = \sum_{i=1}^N c_i \left( \ln \left( \frac{c_i}{c_i^\infty} \right) - 1 \right).$$

The Lyapunov function (2.13) can be reformulated as [51, 64]

$$(2.14) \quad \mathcal{F}[\mathbf{c}] = \sum_{i=1}^N (c_i (\ln c_i - 1) + c_i U_i),$$

where the first part stands for the entropy, and  $U_i$  is the internal energy associated with each species. For the free energy (2.14), the chemical potential associated with

each species can be computed as  $\mu_i(c_i) = \ln c_i + U_i$ . According to the definition of a chemical equilibrium [40], we have  $\sum_{i=1}^N \alpha_i^l \mu_i(c_i^\infty) = \sum_{i=1}^N \beta_i^l \mu_i(c_i^\infty) \forall l$ , which gives the relation between  $U_i$  and  $c_i^\infty$ , i.e.,

$$(2.15) \quad \sum_{i=1}^N \alpha_i^l (\ln c_i^\infty + U_i) = \sum_{i=1}^N \beta_i^l (\ln c_i^\infty + U_i), \quad l = 1, \dots, M.$$

To formulate the reaction kinetics into a variational form, it is important to introduce another state variable  $\mathbf{R} \in \mathbb{R}^M$ , known as the reaction trajectory [54, 64] or the extent of reaction [13, 40]. The  $l$ th component of  $\mathbf{R}(t)$  corresponds to the number of  $l$ th reactions that have happened by time  $t$  in the forward direction. For any initial condition  $\mathbf{c}(0) \in \mathbb{R}_+^N$ , the value of  $\mathbf{c}(t)$  can be represented in terms of  $\mathbf{R}$  as the following formula:

$$(2.16) \quad \mathbf{c}(t) = \mathbf{c}(0) + \boldsymbol{\sigma} \mathbf{R}(t), \quad \boldsymbol{\sigma} \in \mathbb{R}^{N \times M} \text{ is the stoichiometric matrix.}$$

This equation can be viewed as the kinematics of a reaction kinetics, which embodies the conservation properties (2.10). In particular, the positivity of  $\mathbf{c}$  requires a constraint on  $\mathbf{R}$  as follows:

$$\boldsymbol{\sigma} \mathbf{R}(t) + \mathbf{c}(0) > 0.$$

Subsequently, the reaction rate  $\mathbf{r}$  can be defined as  $\dot{\mathbf{R}}$ , known as the reaction velocity [40]. In the framework of the EnVarA, we can describe the reaction kinetics through the energy-dissipation law in terms of  $\mathbf{R}(t)$  and  $\dot{\mathbf{R}}(t)$  as

$$(2.17) \quad \frac{d}{dt} \mathcal{F}[\mathbf{c}(\mathbf{R})] = -\mathcal{D}_{\text{chem}}[\mathbf{R}, \dot{\mathbf{R}}],$$

where  $\mathcal{D}_{\text{chem}}[\mathbf{R}, \dot{\mathbf{R}}]$  is the rate of energy dissipation in the chemical reaction process. Unlike mechanical systems, the rate of energy dissipation for reaction kinetics may not be quadratic in terms of  $\dot{\mathbf{R}}$ , since the system is often far from equilibrium [5, 15]. For a general nonlinear energy dissipation

$$(2.18) \quad \mathcal{D}_{\text{chem}}[\mathbf{R}, \dot{\mathbf{R}}] = \left( \boldsymbol{\Gamma}(\mathbf{R}, \dot{\mathbf{R}}), \dot{\mathbf{R}} \right) = \sum_{l=1}^M \Gamma_l(\mathbf{R}, \dot{\mathbf{R}}) \dot{R}_l \geq 0,$$

since

$$(2.19) \quad \frac{d}{dt} \mathcal{F} = \left( \frac{\delta \mathcal{F}}{\delta \mathbf{R}}, \dot{\mathbf{R}} \right) = \sum_{l=1}^M \frac{\delta \mathcal{F}}{\delta R_l} \dot{R}_l,$$

one can specify

$$(2.20) \quad \Gamma_l(\mathbf{R}, \dot{\mathbf{R}}) = -\frac{\delta \mathcal{F}}{\delta R_l}$$

such that the energy-dissipation law (2.17) holds. Equation (2.20) is the reaction rate equation obtained by an energetic variational approach. It is interesting to note that

$$(2.21) \quad \frac{\delta \mathcal{F}}{\delta R_l} = \sum_{i=1}^N \frac{\delta \mathcal{F}}{\delta c_i} \frac{\delta c_i}{\delta R_l} = \sum_{i=1}^N \sigma_i^l \mu_i,$$

which turns out to be the chemical affinity, and  $\mu_i = \frac{\delta \mathcal{F}}{\delta c_i}$  is the chemical potential of  $i$ th species. The chemical affinity is the driving force of the chemical reaction [13, 14, 40], and the dissipation makes a connection between the reaction rate  $\dot{\mathbf{R}}$  and the chemical affinity. A typical choice of  $\mathcal{D}_{chem}[\mathbf{R}, \dot{\mathbf{R}}]$  is given by

$$(2.22) \quad \mathcal{D}_{chem}[\mathbf{R}, \dot{\mathbf{R}}] = \sum_{l=1}^M \dot{R}_l \ln \left( \frac{\dot{R}_l}{\eta_l(\mathbf{c}(\mathbf{R}))} + 1 \right).$$

One can derive the LMA by taking  $\eta_l(\mathbf{c}(\mathbf{R})) = k_l^- \mathbf{c}(\mathbf{R})^{\beta_l}$ . Since  $\dot{R}_l \approx 0$  near an equilibrium, we see that

$$(2.23) \quad \mathcal{D}_{chem}[\mathbf{R}, \dot{\mathbf{R}}] = \sum_{l=1}^M \dot{R}_l \ln \left( \frac{\dot{R}_l}{\eta_l(\mathbf{c}(\mathbf{R}))} + 1 \right) \approx \sum_{l=1}^M \frac{1}{\eta_l(\mathbf{c}(\mathbf{R}))} \dot{R}_l^2, \quad R_l \ll 1.$$

In turn, the energy-dissipation law (2.17) becomes an  $L^2$ -gradient flow in terms of  $\mathbf{R}$ .

The reaction kinetics can be viewed as a generalized gradient flow, with a non-linear mobility in terms of the reaction trajectory. Hence, it is expected that the numerical techniques for  $L^2$ -gradient flows can be applied to reaction kinetics.

**2.3. EnVarA for reaction-diffusion systems.** For a reaction-diffusion system with  $N$  species and  $M$  reactions, the concentration  $\mathbf{c} \in \mathbb{R}^N$  satisfies the kinematics

$$(2.24) \quad \partial_t c_i + \nabla \cdot (c_i \mathbf{u}_i) = \left( \boldsymbol{\sigma} \dot{\mathbf{R}} \right)_i, \quad i = 1, 2, \dots, N,$$

where  $\mathbf{u}_i$  is the average velocity of each species by its own diffusion, and  $\mathbf{R} \in \mathbb{R}^M$  represents various reaction trajectories involved in the system, with  $\boldsymbol{\sigma} \in \mathbb{R}^{N \times M}$  being the stoichiometric matrix as defined in section 2.1. The equations for  $\mathbf{u}_i$  and  $\dot{\mathbf{R}}$  can be obtained through an energy-dissipation law [7, 64]

$$(2.25) \quad \frac{d}{dt} \mathcal{F}[\mathbf{c}(\mathbf{R})] = -(2\mathcal{D}_{mech} + \mathcal{D}_{chem}),$$

which leads to a reaction-diffusion equation. Here  $\mathcal{F}[\mathbf{c}]$  is the free energy given by

$$(2.26) \quad \mathcal{F}[\mathbf{c}] = \int_{\Omega} \sum_{i=1}^N (c_i (\ln c_i - 1) + c_i U_i) d\mathbf{x},$$

as in (2.14) for the ODE case, and  $2\mathcal{D}_{mech}$  and  $\mathcal{D}_{chem}$  are dissipations for the mechanical and reaction parts, respectively. One key point is that the reaction and diffusion parts of the system dissipate the same free energy. To derive the reaction-diffusion equation (1.1),  $\mathcal{D}_{mech}$  could be taken as

$$2\mathcal{D}_{mech} = \int_{\Omega} \sum_{i=1}^N \xi_i(c_i) |\mathbf{u}_i|^2 d\mathbf{x}, \quad \xi_i(c_i) \text{ is the friction coefficient,}$$

and  $\mathcal{D}_{chem}$  could be taken as

$$\mathcal{D}_{chem} = \int_{\Omega} \sum_{l=1}^M \dot{R}_l \ln \left( \frac{\dot{R}_l}{\eta_l(\mathbf{c}(\mathbf{R}))} + 1 \right) d\mathbf{x}.$$

The energetic variational approach could be applied to the reaction and diffusion parts, respectively. A direct computation shows that the “force balance equations” for the chemical and mechanical subsystems are given by

$$(2.27) \quad \begin{cases} \xi_i(c_i) \mathbf{u}_i = -c_i \nabla \mu_i, & i = 1, 2, \dots, N, \\ \ln \left( \frac{\dot{R}_l}{\eta_l(\mathbf{c}(\mathbf{R}))} \right) = - \sum_{i=1}^N \sigma_i^l \mu_i, & l = 1, \dots, M. \end{cases}$$

In particular, a linear reaction-diffusion system can be obtained by choosing  $\xi_i(c_i) = \frac{1}{D_i} c_i$  as follows:

$$(2.28) \quad \partial_t c_i = D_i \Delta c_i + (\sigma \partial_t \mathbf{R})_i, \quad (\sigma \partial_t \mathbf{R})_i \text{ is the reaction term.}$$

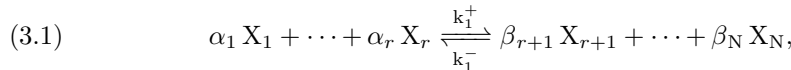
Other choices of  $\xi_i(c_i)$  can result in some porous medium type nonlinear diffusion equation [48]

$$(2.29) \quad \partial_t c_i = \nabla \cdot (D(c_i) \nabla c_i) + (\sigma \partial_t \mathbf{R})_i,$$

where  $D(c_i) = \frac{c_i}{\eta(c_i)}$  is the concentration-dependent diffusion coefficient.

In this formulation, the reaction part is reformulated in terms of reaction trajectories  $R$ , and the reaction and diffusion parts impose different dissipation mechanisms for the same physical energy.

**3. The second-order operator splitting scheme.** In this section, we construct a second-order operator splitting scheme to a reaction-diffusion system based on the energetic variational formulation outlined in section 2.3, in which the numerical discretization for the reaction part is applied to the reaction trajectory  $R$  in the reaction space, while the numerical method for the diffusion part is designed for the concentration  $\mathbf{c}$  in the species space. To illustrate the idea, we focus on a case with one reversible detailed balance reaction, given by



where  $k_1^+$  and  $k_1^-$  are constants. Moreover, we assume that the reaction-diffusion system can be derived from an energy-dissipation law (2.25). Numerical schemes for systems involving multiple reversible reactions can be constructed in the same manner, although the theoretical justifications, especially the unique solvability, might be difficult to establish.

To simplify the numerical description, the reaction-diffusion equation (2.29) can be rewritten as

$$(3.2) \quad \partial_t \mathbf{c} = \mathcal{A} \mathbf{c} + \mathcal{B} \mathbf{c},$$

where  $\mathcal{A}$  is a reaction operator and  $\mathcal{B}$  is a diffusion operator. Throughout this section, the computational domain is taken as  $\Omega = (0, 1)^3$  with a periodic boundary condition, and  $\Delta x = \Delta y = \Delta z = h = \frac{1}{N_0}$  with  $N_0$  being the spatial mesh resolution; a computational domain with a different boundary condition or numerical mesh could be analyzed in a similar fashion. In addition, the discrete free energy is defined as follows, with the given spatial discretization:

$$(3.3) \quad \mathcal{F}_h(\mathbf{c}) := \left\langle \sum_{i=1}^N (c_i (\ln c_i - 1) + c_i U_i), \mathbf{1} \right\rangle,$$

where  $\langle f, g \rangle = h^3 \sum_{i,j,k=0}^{N_0-1} f_{i,j,k} g_{i,j,k}$  denotes the discrete  $L^2$  inner product.

Following the second-order Strang splitting formula  $\mathbf{c}^{n+1} = e^{\frac{1}{2}\Delta t \mathcal{A}} e^{\Delta t \mathcal{B}} e^{\frac{1}{2}\Delta t \mathcal{A}} \mathbf{c}^n$  [62], the numerical solution  $\mathbf{c}^{n+1}$  can be obtained through three stages. Given  $\mathbf{c}^n$  with  $c_{i,j,k}^n \in \mathbb{R}_+^N$ , we update  $\mathbf{c}^{n+1}$  via the following three stages.

**Stage 1.** First, we set  $\mathbf{c}_0 = \mathbf{c}^n$  and solve the reaction trajectory equation, subject to the initial condition  $R^n = 0$ , with a second-order, positivity-preserving, energy stable scheme, with the temporal step-size  $\Delta t/2$ . An intermediate numerical profile is updated as

$$(3.4) \quad \mathbf{c}^{n+1,(1)} = \mathbf{c}^n + \boldsymbol{\sigma} R^{n+1,(1)}.$$

**Stage 2.** Starting with the intermediate variable  $\mathbf{c}^{n+1,(1)}$ , we solve the diffusion equation  $\partial_t \mathbf{c} = \mathcal{B} \mathbf{c}$  by a second-order, positivity-preserving, and energy stable scheme with the temporal step-size  $\Delta t$  to obtain  $\mathbf{c}^{n+1,(2)}$ .

**Stage 3.** We set  $\mathbf{c}_0 = \mathbf{c}^{n+1,(2)}$  and repeat Stage 1, i.e., solving the reaction trajectory equation, subject to the initial condition  $R^n = 0$  with the temporal step-size  $\Delta t/2$  to obtain  $R^{n+1,(2)}$ . The numerical solution at  $t^{n+1}$  is updated as

$$(3.5) \quad \mathbf{c}^{n+1} = \mathbf{c}^{n+1,(2)} + \boldsymbol{\sigma} R^{n+1,(2)}.$$

More details of the numerical algorithms at each stage will be provided in the following subsections.

**3.1. Second-order algorithm for reaction kinetics.** We first develop a second-order algorithm for the reaction stage, which only needs to be constructed in a point-wise sense. The discrete free energy can be reformulated in terms of  $R$  at each mesh point, and is denoted by

$$(3.6) \quad F(R) = \sum_{i=1}^N c_i(R) (\ln c_i(R) - 1) + c_i(R) U_i.$$

For simplicity of presentation, we omit the grid index throughout this subsection. Following the earlier discussions, for a given initial condition  $\mathbf{c}^0$ , the reaction trajectory equation is given by

$$(3.7) \quad \begin{cases} \ln \left( \frac{R_t}{\eta(\mathbf{c}(R))} + 1 \right) = -\mu(R), \\ \mu(R) = \frac{\delta F}{\delta R} = \sum_{i=1}^N \sigma_i \mu_i(c_i(R)), \end{cases}$$

where  $\eta(\mathbf{c}(R))$  is the nonlinear mobility that takes the form  $\eta(\mathbf{c}(R)) = k_1^- \prod_{i=r+1}^N c_i^{\beta_i}$ ,  $\mathbf{c}(R) = \mathbf{c}^0 + \boldsymbol{\sigma} R$  with  $\boldsymbol{\sigma} = (-\alpha_1, -\alpha_2, \dots, -\alpha_r, \beta_1, \beta_2, \dots, \beta_N)^\top$  is the stoichiometric vector, and  $\mu_i(c_i) = \ln c_i + U_i$  is the chemical potential associated with  $i$  species. Similar to an  $L^2$ -gradient flow, a second-order algorithm for the reaction trajectory equation (3.7) can be constructed through a Crank–Nicolson type discretization

$$(3.8) \quad \ln \left( \frac{R^{n+1} - R^n}{\eta(\mathbf{c}(R^*)) \Delta t} + 1 \right) = -\mu^{n+1/2},$$

where  $\mu^{n+1/2}$  is a suitable approximation to the chemical affinity,  $F'(R)$ , at  $t_{n+1/2}$ , and  $R^*$  is an approximation to  $R^{n+1/2}$ , which needs to be independent of  $R^{n+1}$ . The primary difficulty is focused on the construction of  $R^*$  and  $\mu^{n+1/2}$  to ensure the unique solvability as well as the positivity of  $R^{n+1} - R^n + \eta(\mathbf{c}(R^*)) \Delta t$  and  $\mathbf{c}(R^{n+1})$ .

First, we use a first-order scheme to obtain a rough “guess” to  $R^{n+1}$ , denoted by  $\widehat{R}^{n+1}$ , as a numerical solution to

$$(3.9) \quad \ln \left( \frac{\widehat{R}^{n+1} - R^n}{\eta(\mathbf{c}(R^n))\Delta t} + 1 \right) = \sum_{i=1}^N \sigma_i \mu_i(\widehat{R}^{n+1})$$

in the admissible set. This first-order scheme was proposed in [45], while the unique solvability and the positivity-preserving property have been proved. With  $\widehat{R}^{n+1}$  at hand, we introduce  $R^* = (R^n + \widehat{R}^{n+1})/2$ . Although (3.9) corresponds to a first-order truncation error, we see that  $\widehat{R}^{n+1}$  is a second-order approximation to  $R^{n+1}$ , locally in time, due to the  $\Delta t$  term in the denominator. In turn,  $R^*$  becomes a second-order approximation to  $R^{n+1/2}$ . To approximate  $(\frac{\delta \mathcal{F}}{\delta R})^{n+1/2}$ , we apply the idea of the **discrete variational derivative method** [23, 27]. More specifically, the function

$$(3.10) \quad \phi(p, q) = \begin{cases} \frac{F(p)-F(q)}{p-q}, & p \neq q, \\ F'(p), & p = q, \end{cases}$$

is introduced as a second-order approximation to  $F'(\frac{p+q}{2})$ . In fact, it is also known as the discrete variation of  $F(R)$  [27].

With the combined arguments, the second-order algorithm is constructed as

$$(3.11) \quad \begin{cases} \ln \left( \frac{R^{n+1} - R^n}{\eta(\mathbf{c}(\widehat{R}^{n+1/2}))\Delta t} + 1 \right) = -\mu_R^{n+1/2}, & \widehat{R}^{n+1/2} = \frac{1}{2}(R^n + \widehat{R}^{n+1}), \\ \mu_R^{n+1/2} = \phi(R^{n+1}, R^n) + \Delta t \sum_{i=1}^N \sigma_i (\mu_i(R^{n+1}) - \mu_i(R^n)). \end{cases}$$

The term  $\Delta t \sum_{i=1}^N \sigma_i (\mu_i(R^{n+1}) - \mu_i(R^n))$  is the Douglas–Dupont type regularization term [10], which is added for the theoretical analysis of the positivity-preserving property. This  $O(\Delta t^2)$  term is artificial, and it will not affect the second-order accuracy in the temporal discretization.

This algorithm can be reformulated as an optimization problem

$$(3.12) \quad \begin{cases} R = \arg \min_{R \in \mathcal{V}_n} J_n(R), \\ J_n(R) = \Psi_n(R, R^n) + \int_{R^n}^R \phi(s, R^n) ds + \lambda(\Delta t F(R) - (\gamma^n, R)), \\ \mathcal{V}_n = \left\{ R \mid c_i(R) > 0, \quad R - R^n + \eta(\mathbf{c}(\widehat{R}^{n+1/2}))\Delta t > 0 \right\}, \end{cases}$$

where  $\gamma^n = \Delta t \sum_{i=1}^N \sigma_i \mu_i(c_i(R^n))$ , and

$$(3.13) \quad \Psi_n(R, R^n) = (R - R^n + \eta(\mathbf{c}(\widehat{R}^{n+1/2}))\Delta t) \ln \left( \frac{R - R^n}{\eta(\mathbf{c}(\widehat{R}^{n+1/2}))\Delta t} + 1 \right) - (R - R^n)$$

is a function that measures the “distance” between  $R$  and  $R^n$ . Although an explicit form of  $J_n(R)$  is not available, we can prove that  $J_n(R)$  admits a unique minimizer in the admissible set. More precisely, the following theorem is valid.

**THEOREM 3.1.** *Given  $\mathbf{c}^n > 0$  and  $R^n = 0$ , there exists a unique solution  $R^{n+1}$  for the minimization problem (3.12), which turns out to be the unique solution for the numerical scheme (3.11), with  $\mathbf{c}(R^{n+1}) > 0$  and  $R^{n+1} + \eta(\mathbf{c}(\widehat{R}^{n+1/2}))\Delta t > 0$ . Therefore, the numerical scheme is well defined.*

To facilitate the proof of this result, the following smooth functions are introduced for fixed  $a > 0$ :

$$\begin{aligned}
 (3.14) \quad G_a^1(x) &= \frac{x \ln x - a \ln a}{x - a}, \\
 G_a^0(x) &= \int_a^x G_a^1(s) ds, \\
 G_a^2(x) &= (G_a^0)''(x) = (G_a^1)' = \frac{x - a + a(\ln a - \ln x)}{(x - a)^2}.
 \end{aligned}$$

By a direct calculation, it is straightforward to prove the following results, which will be used in the proof of Theorem 3.1.

LEMMA 3.1. *For any fixed  $a > 0$ , we have that (1)  $G_a^2(x) \geq 0$  for any  $x > 0$ ; (2)  $G_a^0(x)$  is convex in terms of  $x$ ; (3) there exists  $\xi$  between  $a$  and  $x$  such that  $(G_a^1)'(x) = \frac{1}{\xi}$ ; and (4) since  $G_a^1(x)$  increases in terms of  $x$ , we have  $G_a^1(x) \leq G_a^1(a)$  for any  $0 < x \leq a$ .*

Now we can proceed to the proof of Theorem 3.1.

*Proof.* Recall the minimization problem (3.12); it is clear that  $J_n(R)$  is a strictly convex function over  $\mathcal{V}_n$ . We need only prove that the minimizer of  $J_n(R)$  over  $\mathcal{V}$  could not occur on the boundary of  $\mathcal{V}$ , so that a minimizer corresponds to a numerical solution of (3.11) in  $\mathcal{V}_n$ .

The following closed domain is considered in the analysis:

$$(3.15) \quad \mathcal{V}_\delta = \left\{ R \mid c_i(R) \geq \delta, \quad R - R^n + \eta(c(\hat{R}^{n+1/2}))\Delta t \geq \delta \right\} \subset \mathcal{V}.$$

A careful calculation indicates that, for any  $R \in \mathcal{V}_\delta$ , the following bounds are satisfied:

$$(3.16) \quad \max \frac{1}{\beta_i}(\delta - c_i^0) \leq R \leq \min \frac{1}{\alpha_i}(c_i^0 - \delta), \quad R \geq R^n - \eta(c(\hat{R}^{n+1/2}))\Delta t + \delta,$$

i.e.,  $\mathcal{V}_\delta = [\max \frac{1}{\beta_i}(\delta - c_i^0), \min \frac{1}{\alpha_i}(c_i^0 - \delta)]$  or  $\mathcal{V}_\delta = [R^n - \eta(c(\hat{R}^{n+1/2}))\Delta t + \delta, \min \frac{1}{\alpha_i}(c_i^0 - \delta)]$ . Since  $\mathcal{V}_\delta$  is a bounded, compact set, there exists a (may not be unique) minimizer of  $J_n(R)$  over  $\mathcal{V}_\delta$ . Moreover, we have to prove that such a minimizer could not occur on the boundary points in  $\mathcal{V}_\delta$  if  $\delta$  is sufficiently small; we do so by using the singular property of logarithmic function approaches to 0.

Without loss of generality, the minimization point is assumed to be  $R^* = R^n - \eta(c(\hat{R}^{n+1/2}))\Delta t + \delta$ . A direct calculation gives

$$(3.17) \quad J'_n(R) |_{R=R^*} = \ln \delta + \phi(R^*, R^n) + \Delta t(\mu(R^*) - \gamma^n).$$

Next, we show that  $\phi(R^*, R^n) + \Delta t(\mu(R^*) - \gamma^n)$  is bounded, so that we can choose  $\delta$  sufficiently small with

$$(3.18) \quad J'_n(R) |_{R=R^*} < 0,$$

which leads to a contradiction since there will be  $R^{*'} = R^n - \eta(c(\hat{R}^{n+1/2}))\Delta t + \delta + \delta' \in \mathcal{V}_\delta$  such that

$$(3.19) \quad J_n(R^{*'}) < J_n(R^*).$$

To derive a bound for  $\phi(R^*, R^n) + \Delta t(\mu(R^*) - \gamma^n)$ , we note that

$$(3.20) \quad \phi(R^*, R^n) = \sum_{i=1}^N \sigma_i G_{c_i^n}^1(c_i^0 + \sigma_i R^*) + \sum_{i=1}^N \sigma_i (U_i - 1),$$

where  $c_i^n = c_i^0 + \sigma_i R^n$ , and  $\sum_{i=1}^N \sigma_i (U_i - 1)$  is a constant. Since  $G_a^1(x)$  is an increasing function of  $x$  for any  $a > 0$ , the following inequality is valid:

$$(3.21) \quad \begin{aligned} G_{c_i^n}^1(c_i^0 + \sigma_i R^*) &= G_{c_i^n}^1(c_i^0 + \sigma_i (R^n - \hat{\eta}^{n*} \Delta t - \delta)) = G_{c_i^n}^1(c_i^0 + \sigma_i R^n - \sigma_i (\hat{\eta}^{n*} \Delta t - \delta)) \\ &\geq G_{c_i^n}^1(c_i^0 + \sigma_i R^n) = \ln c_i^n + 1, \quad \sigma_i < 0, \end{aligned}$$

in which  $\delta$  is sufficiently small such that  $\hat{\eta}^{n*} \Delta t - \delta > 0$ . Similarly, we have

$$(3.22) \quad G_{c_i^n}^1(c_i^0 + \sigma_i R^*) \leq G_{c_i^n}^1(c_i^0 + \sigma_i R^n) = \ln c_i^n + 1, \quad \sigma_i > 0,$$

with  $\delta$  sufficiently small such that  $\hat{\eta}^{n*} \Delta t - \delta > 0$ . Hence,

$$(3.23) \quad \begin{aligned} \phi(R^*, R^n) &= \sum_{i=1}^N \sigma_i G_{c_i^n}^1(c_i^0 + \sigma_i R^*) + \sum_{i=1}^N \sigma_i (U_i - 1) \\ &\leq \sum_{i=1}^N \sigma_i \ln c_i^n + C_0, \quad C_0 = \sum_{i=1}^N \sigma_i U_i. \end{aligned}$$

Following the same argument, we could derive the inequality

$$(3.24) \quad \begin{aligned} \mu(R^*) &= \sum_{i=1}^N \sigma_i \mu_i(c_i + \sigma_i R^*) = \sum_{i=1}^N \sigma_i \ln(c_i^0 + \sigma_i R^*) + \sum_{i=1}^N \sigma_i U_i \\ &\leq \sigma_i \ln(c_i^n) + C_0, \end{aligned}$$

since  $\ln x$  is an increasing function of  $x$ . A combination of (3.23) and (3.24) gives

$$(3.25) \quad J'_n(R) |_{R=R^*} \leq \ln \delta + C_1,$$

where  $C_i = (1 + \Delta t) \sum_{i=1}^N \sigma_i \ln(c_i^n) + (1 + \Delta t)C_0 - \Delta t\gamma^n$  is a constant. So we can choose  $\delta$  small enough such that  $J'_n(R) |_{R=R^*} < 0$ , which leads to the contradiction inequality (3.19).

Using similar arguments, if  $R^* = \min \frac{1}{\alpha_i}(c_i^0 - \delta) = \frac{1}{\alpha_q}(c_q^0 - \delta)$ , we can prove that

$$(3.26) \quad J'_n(R) |_{R=R^*} \geq C_2 + \Delta t(-\alpha_q) \ln \delta.$$

Then  $\delta$  can be chosen sufficiently small such that  $J'_n(R) |_{R=R^*} > 0$ , which leads to a contradiction. Meanwhile, if  $R^* = \max \frac{1}{\beta_i}(\delta - c_i^0)$ , we will have  $J'_n(R) |_{R=R^*} < 0$ .

As a result, the global minimum of  $J_n(R)$  over  $V_\delta$  could only possibly occur at an interior point if  $\delta$  is sufficiently small. In turn, there is a minimizer  $R^* \in (V_\delta)^\circ$  in the interior region  $V_\delta$  of  $J_n(R^*)$ , so that  $J'_n(R) = 0$ . In other words,  $R^*$  has to be the numerical solution of (3.11), provided that  $\delta$  is sufficiently small. Therefore, the existence of a “positive” numerical solution is proved. In addition, since  $J(R)$  is a strictly convex function over  $V$ , the uniqueness of this numerical solution follows from a standard convexity analysis. The proof of Theorem 3.1 is finished.  $\square$

The energy stability of the numerical scheme (3.11) is stated below.

**THEOREM 3.2.** *For a given  $R^n$ , the numerical solution  $R^{n+1}$  to (3.11) satisfies the energy-dissipation estimate*

$$(3.27) \quad F(R^{n+1}) \leq F(R^n) \quad \text{at a pointwise level.}$$

*Proof.* Multiplying both side of (3.11) by  $R^{n+1} - R^n$  and rearranging terms yields

$$(3.28) \quad \begin{aligned} \frac{F(R^{n+1}) - F(R^n)}{\Delta t} &= -\frac{R^{n+1} - R^n}{\Delta t} \ln \left( \frac{R^{n+1} - R^n}{\eta(\mathbf{c}(\widehat{R}^{n+1/2}))\Delta t} + 1 \right) \\ &\quad - \sum_{i=1}^N \sigma_i (\mu_i^{n+1} - \mu_i^n) (R^{n+1} - R^n) \\ &\leq -\frac{R^{n+1} - R^n}{\Delta t} \ln \left( \frac{R^{n+1} - R^n}{\eta(\mathbf{c}(\widehat{R}^{n+1/2}))\Delta t} + 1 \right) \leq 0. \end{aligned}$$

In the derivation of the above inequality, the following fact has been used:

$$(3.29) \quad \sigma_i (\mu_i^{n+1} - \mu_i^n) (R^{n+1} - R^n) = \sigma_i (\ln(c_i^0 + \sigma_i R^{n+1}) - \ln(c_i^0 + \sigma_i R^n)) (R^{n+1} - R^n) \geq 0,$$

which comes from the monotonic property of the logarithmic function.  $\square$

*Remark 3.1.* Without the additional term  $\Delta t \sum_{i=1}^N \sigma_i (\mu_i(R^{n+1}) - \mu_i(R^n))$ , the discrete energy dissipation law (3.28) is an exact time discretization to the continuous energy-dissipation law, which is the advantage of the discrete variational derivative method. It is crucial to add this term to establish the positivity-preserving property of the numerical solution in the admissible set. Also see the related numerical analysis for the Cahn–Hilliard gradient flow with Flory–Huggins energy potential [10, 18, 19, 20], and the Poisson–Nernst–Planck (PNP) system [47, 59].

*Remark 3.2.* There have been extensive works of second-order accurate, energy stable numerical schemes to various gradient flows, based on either the modified Crank–Nicolson [1, 2, 17, 31, 35, 61] or the BDF2 [42, 66] approach. Meanwhile, most existing works are multistep methods, since a multistep approximation to the concave terms is usually needed to ensure both the unique solvability and the energy stability. However, for the operator splitting method, a single-step, second-order approximation has to be accomplished at each stage, so that these standard approaches are not directly available. To overcome this difficulty, we construct a numerical profile  $\widehat{R}^{n+1}$ , a local-in-time second-order approximation of  $R$  at time step  $t^{n+1}$ , so that a multistep approximation to the mobility function is avoided. In addition, the fact that the physical energy does not contain any concave part enables one to derive a single-step, modified Crank–Nicolson method while preserving the energy stability. Recently, some single-step, second-order accurate, and energy stable schemes for gradient flow problems have been developed, based on a second-order exponential time differencing Runge–Kutta method (ETDRK2) [21, 26]. This approach may also be used to develop second-order, energy stable schemes to reaction-diffusion systems, which will be explored in future work.

**3.2. Second-order schemes in the diffusion stage.** Since the cross-diffusion is not considered, the  $N$  diffusion equations of  $c_i$  are fully decoupled. Therefore, we need only construct numerical algorithms for a diffusion equation

$$(3.30) \quad \rho_t = \nabla \cdot (D(\rho, \mathbf{x}) \nabla \rho), \quad D(\rho, \mathbf{x}) \text{ is the diffusion coefficient.}$$

In this subsection, we present two positivity-preserving and energy stable numerical algorithms for linear and nonlinear diffusion equations, respectively. The schemes could be used in the diffusion stage for the operator splitting scheme.

The diffusion equation (3.30) satisfies an energy-dissipation law

$$(3.31) \quad \int \rho \ln \rho + C \rho d\mathbf{x} = - \int \mathcal{M}(\rho, \mathbf{x}) |\nabla \mu|^2 d\mathbf{x},$$

where  $\mathcal{M}(\rho, \mathbf{x}) = D(\rho, \mathbf{x})\rho$  is known as the mobility,  $C$  is an arbitrary constant, and  $\nabla \mu = \nabla(\ln \rho)$  turns out to be the gradient of the chemical potential  $\mu = \rho \ln \rho + C\rho + 1$ . With a careful spatial discretization, the discrete energy is defined as

$$(3.32) \quad \mathcal{F}_h(\rho) := \langle \rho \ln \rho + C\rho, \mathbf{1} \rangle.$$

**3.2.1. An exponential time differencing scheme for a linear diffusion.**

We first consider a linear diffusion with a constant coefficient, given by

$$(3.33) \quad \rho_t = \mathcal{L}\rho, \quad \mathcal{L} = D\Delta, \quad D > 0,$$

subject to the periodic boundary condition. Of course, the solution of linear diffusion equation (3.33) satisfies the following maximum principle:

$$(3.34) \quad \max_{\Omega} \rho(\mathbf{x}, t) \leq \max_{\Omega} \rho(\mathbf{x}, 0), \quad \min_{\Omega} \rho(\mathbf{x}, t) \geq \min_{\Omega} \rho(\mathbf{x}, 0) \quad \forall t > 0.$$

An easy way to obtain a high-order scheme to a linear diffusion equation is to apply the ETD method [12, 39], which is indeed exact in time. More precisely, we can introduce the spatial discretization to (3.33) by the standard centered difference method, which leads to

$$(3.35) \quad \partial_t \rho = \mathcal{L}_h \rho.$$

Integrating the above equation over a single time step from  $t = t_n$  to  $t_{n+1}$ , we get

$$(3.36) \quad \rho^{n+1} = e^{\mathcal{L}_h \Delta t} \rho^n,$$

which is known as the ETD scheme [12].

Due to the discrete maximum principle [22], the following positivity-preserving property is obvious.

**THEOREM 3.3.** *Given  $\rho^n$ , with  $\rho_{i,j,k}^n > 0$ ,  $0 \leq i, j, k \leq N_0 - 1$ , there exists a unique solution  $\rho^{n+1}$  for the numerical scheme (3.36), with the discrete periodic boundary condition, with  $\rho_{i,j,k}^{n+1} > 0$ ,  $0 \leq i, j, k \leq N_0 - 1$ .*

With the positivity-preserving property and unique solvability for the numerical scheme (3.36), it is straightforward to prove an unconditional energy stability.

**THEOREM 3.4.** *For the numerical solution (3.36), we have*

$$(3.37) \quad \mathcal{F}_h(\rho^{n+1}) \leq \mathcal{F}_h(\rho^n),$$

so that  $\mathcal{F}_h(\rho^n) \leq \mathcal{F}_h(\rho_h^0)$ , an initial constant.

*Proof.* Taking a discrete inner product with (3.35) by  $\ln \rho$  gives

$$(3.38) \quad \left\langle \frac{d}{dt} \rho, \ln \rho \right\rangle = - \langle \nabla_h \rho, \nabla_h(\ln \rho) \rangle.$$

By a direct calculation, we have

$$(3.39) \quad \frac{d}{dt} \mathcal{F}_h(\rho) = \left\langle \frac{d}{dt} \rho, \ln \rho \right\rangle = -\langle \nabla_h \rho, \nabla_h(\ln \rho) \rangle \leq 0,$$

where the last inequality is due to the monotone property of the logarithmic function. This completes the proof.  $\square$

In fact, such a stability is available not only for  $\mathcal{F}_h(\rho)$  given by (3.32), but also for all the convex energies. The following estimate could be derived using similar techniques.

**COROLLARY 3.1.** *For the numerical solution (3.35), we have  $\mathcal{F}_h(\rho^{n+1}) \leq \mathcal{F}_h(\rho^n)$  for any  $n \geq 0$ , and  $\mathcal{F}_h(\rho)$  taking the form*

$$\mathcal{F}(\rho) = \langle F(u), \mathbf{1} \rangle, \quad \text{in which } F \text{ is a convex function of } \rho \text{ for } \rho > 0.$$

**3.2.2. Second-order scheme for a nonlinear diffusion equation.** The ETD scheme is not suitable for nonlinear diffusion equations. The construction of a second-order accurate, positivity-preserving, and energy stable scheme for a generalized nonlinear diffusion equation has always been very challenging. Here we present a general approach to achieve this goal. For simplicity of presentation, it is assumed that the diffusion coefficient  $D(\rho)$  depends only explicitly on  $\rho$ . The case of  $\mathbf{x}$ -dependent coefficients could be handled in a similar manner.

The idea is quite similar to the scheme (3.11) in the reaction stage. First, we need a rough guess  $\hat{\rho}^{n+1}$ , which has to be pointwise positive, as a second-order temporal approximation to  $\rho^{n+1}$ . The simplest way to obtain such a rough guess  $\hat{\rho}^{n+1}$  is to use the classical semi-implicit scheme

$$(3.40) \quad \frac{\hat{\rho}^{n+1} - \rho^n}{\Delta t} = \nabla_h \cdot \left( \mathcal{A}_h[D(\rho^n)] \nabla_h \hat{\rho}^{n+1, (2)} \right),$$

where  $\nabla_h$  and  $\nabla_h \cdot$  stand for the discrete gradient and the discrete divergence, respectively, and  $\mathcal{A}_h[D(\rho^n)]$  is a spatially averaging operator introduced to obtain the value of  $D(\rho^n)$  at staggered mesh points. As proved in a recent work, the semi-implicit scheme (3.40) satisfies the following uniquely solvable and positivity-preserving properties.

**PROPOSITION 3.1** (see [45]). *Given  $\rho^n$ , with  $\rho_{i,j,k}^n > 0$ ,  $0 \leq i, j, k \leq N_0$ , there exists a unique solution  $\rho^{n+1}$  for the numerical scheme (3.40), with the discrete periodic boundary condition, with  $\rho_{i,j,k}^{n+1} > 0$ ,  $0 \leq i, j, k \leq N_0$ .*

It is observed that, although the truncation error for (3.40) is only  $O(\Delta t)$  in the temporal discretization, a single-step computation would lead to an  $O(\Delta t^2)$  approximation to the PDE solution of  $\rho_t = \mathcal{B}\rho$  at time step  $t^{n+1}$ , as long as  $\rho^n$  retains a second-order temporal accuracy. Within the rough guess  $\hat{\rho}^{n+1}$ , we define  $\hat{\rho}^{n+1/2} = \frac{1}{2}(\rho^n + \hat{\rho}^{n+1})$ , which is an  $O(\Delta t^2)$  approximation to  $\rho$  at the time instant  $t^{n+1/2}$ . Thus, a second-order accurate scheme can be constructed through a Crank–Nicolson type discretization, along with the discrete variational derivative method [23, 27]

$$(3.41) \quad \begin{cases} \frac{\rho^{n+1} - \rho^n}{\Delta t} = \nabla_h(\mathcal{M}_h^{n+1/2}) \nabla_h \mu^{n+1/2}, \\ \mu^{n+1/2} = \frac{F(\rho^{n+1}) - F(\rho^n)}{\rho^{n+1} - \rho^n} + \Delta t(\ln \rho^{n+1} - \ln \rho^n), \\ \mathcal{M}_h^{n+1/2} = \mathcal{A}_h(D(\hat{\rho}^{n+1/2}) \hat{\rho}^{n+1/2}), \end{cases}$$

where  $F(\rho) = \rho \ln \rho + C\rho$  is the free energy density. Similar to the derivation of (3.11), the artificial regularization term  $\Delta t(\ln \rho^{n+1} - \ln \rho^n)$ , which does not affect the overall accuracy, is needed in the theoretical justification of the positivity-preserving property; see the following theorem.

**THEOREM 3.5.** *Given  $\rho^n$ , with  $\rho_{i,j,k}^n > 0 \forall 0 \leq i, j, k \leq N_0 - 1$ , there exists a unique solution  $\rho^{n+1}$  for the numerical scheme (3.41), with the discrete periodic boundary condition satisfying  $\rho_{i,j,k}^{n+1} > 0$ .*

To simplify notation, we introduce an average operator,

$$\bar{f} = \frac{h^3}{|\Omega|} \sum_{i,j,k=0}^{N-1} f_{i,j,k},$$

and define a hyperplane in  $R^{N_0^3}$ , with dimension  $(N_0^3 - 1)$ ,

$$(3.42) \quad H = \left\{ \rho_{i,j,k} = \beta_0 + \psi_{i,j,k} : \sum_{i,j,k=0}^{N_0-1} \psi_{i,j,k} = 0 \right\}.$$

Meanwhile, we recall a preliminary estimate, which has been proved in a recent work [10]. Let  $\mathcal{C}_\Omega$  be the space of grid functions on  $\Omega$ . For any

$$(3.43) \quad \varphi \in \mathring{\mathcal{C}}_\Omega = \{ \nu \in \mathcal{C}_\Omega \mid \bar{\nu} = 0 \},$$

there exists a unique  $\xi \in \mathring{\mathcal{C}}_\Omega$  that solves

$$(3.44) \quad \mathcal{L}_{\mathcal{M}}(\xi) = \varphi, \quad \text{where } \mathcal{L}_{\mathcal{M}}(\xi) := -\nabla_h \cdot (\tilde{\mathcal{M}} \nabla_h \xi).$$

In turn, we can define the discrete norm

$$(3.45) \quad \|\varphi\|_{\mathcal{L}_{\mathcal{M}}^{-1}} = \sqrt{\langle \varphi, \mathcal{L}_{\mathcal{M}}^{-1}(\varphi) \rangle},$$

which is a discrete weighted  $H^{-1}$ -norm associated with a nonconstant mobility.

**LEMMA 3.2** (see [10]). *Suppose that  $\varphi_1, \varphi_2 \in \mathcal{C}_{\text{per}}$ , with  $\langle \varphi_1 - \varphi_2, \mathbf{1} \rangle = 0$ , i.e.,  $\varphi_1 - \varphi_2 \in \mathring{\mathcal{C}}_{\text{per}}$ , and assume that  $\|\varphi_1\|_\infty, \|\varphi_2\|_\infty \leq M_h$ , and  $\mathcal{M} \geq \mathcal{M}_0$  at a pointwise level. Then we have the inequality*

$$(3.46) \quad \|\mathcal{L}_{\mathcal{M}}^{-1}(\varphi_1 - \varphi_2)\|_\infty \leq C_2 := \tilde{C}_2 \mathcal{M}_0^{-1} h^{-1/2},$$

where  $\tilde{C}_2 > 0$  depends only upon  $\mathcal{M}_h$  and  $\Omega$ .

Now we proceed to the proof of Theorem 3.5.

*Proof.* The mass conservation property of the numerical solution (3.41) is obvious:

$$(3.47) \quad \overline{\rho^{n+1}} = \overline{\rho^n} := \beta_0.$$

A direct calculation implies that if  $\rho^{n+1}$  with  $\rho_{i,j,k}^{n+1} > 0$  is the numerical solution of (3.41), then  $\rho^{n+1}$  is a minimization of the discrete energy functional

$$(3.48) \quad J_n(\rho) = \frac{1}{2\Delta t} \|\rho - \rho^n\|_{\mathcal{L}_{\mathcal{M}^n}^{-1}} + \langle G_{\rho^n}^0(\rho) + \Delta t(\rho \ln \rho + C_n \rho), \mathbf{1} \rangle$$

over the admissible set

$$(3.49) \quad V_h^H := \{ \rho = \beta_0 + \psi \mid \bar{\psi} = 0, 0 < \rho_{i,j,k} < M_h \forall (i, j, k) \}.$$

Here  $C_n = C - 1 - \Delta t(1 + \ln \rho^n)$ ,  $G_{\rho^n}^0(\rho)$  is defined as in (3.14), and  $M_h = \frac{\beta_0}{h^3}$ .

To this end, we consider the following closed domain:

$$(3.50) \quad V_{h,\delta}^H = \{\psi : \bar{\psi} = 0, \delta \leq \rho_{i,j,k} \leq M_h\} \subset V_h^H.$$

Since  $V_{h,\delta}^H$  is a bounded, compact set in the hyperplane  $H$ , there exists a (may not be unique) minimizer of  $J_h(\psi)$  over  $V_{h,\delta}^H$ . The key point of the positivity analysis is that such a minimizer could not occur on the boundary points (in  $H$ ) if  $\delta$  is small enough.

For a given  $\rho^n$  with  $\rho_{i,j,k}^n > 0$ , we can assume that  $\rho^n$  satisfies the following bounds:

$$(3.51) \quad \epsilon_0 \leq \rho_{i,j,k}^n \leq M_h - \epsilon_0 \quad \forall 0 \leq i, j, k \leq N_0 - 1.$$

Assume a minimizer of  $J_n(\rho)$  occurs at a boundary point of  $V_{h,\delta}^H$ . Without loss of generality, we set the minimization point as  $\rho_{i,j,k}^*$ , with  $\rho_{i_0,j_0,k_0}^* = \delta$ . In addition, we denote the grid point at which  $\rho^*$  reaches the maximum value as  $(i_1, j_1, k_1)$ . It is obvious that  $\rho_{i_1,j_1,k_1}^* \geq \beta_0$ , because of the fact that  $\bar{\rho}^* = \beta_0$ .

To obtain a contradiction, we compute the direction derivative of  $J_n(\rho)$  along the direction

$$(3.52) \quad \delta\psi = \delta_{i,i_0}\delta_{j,j_0}\delta_{k,k_0} - \delta_{i,i_1}\delta_{j,j_1}\delta_{k,k_1} \in \mathring{C}_{\text{per}}, \quad \delta_{k,l} \text{ is the Kronecker delta function,}$$

and the following identity is valid:

$$\begin{aligned} \frac{1}{h^3} \frac{J_n(\rho^* + s\delta\psi) - J_n(\rho^*)}{s} \Big|_{s=0} &= \frac{1}{\Delta t} ((\mathcal{L}_{\check{\mathcal{M}}^n}(\rho^* - \rho^n))_{i_0,j_0,k_0} - (\mathcal{L}_{\check{\mathcal{M}}^n}(\rho^* - \rho^n))_{i_1,j_1,k_1}) \\ &+ (G_{\rho^n}^1(\rho^*))_{i_0,j_0,k_0} - (G_{\rho^n}^1(\rho^*))_{i_1,j_1,k_1} + \Delta t(\ln \rho_{i_0,j_0,k_0}^* - \ln \rho_{i_1,j_1,k_1}^*) + \langle C_n, \delta\psi \rangle. \end{aligned}$$

In addition, by the facts that  $\rho_{i_0,j_0,k_0}^* = \delta$  and  $\rho_{i_1,j_1,k_1}^* \geq \beta_0$ , we get

$$(3.53) \quad \ln \rho_{i_0,j_0,k_0}^* - \ln \rho_{i_1,j_1,k_1}^* \leq \ln \delta - \ln \beta_0.$$

In the meantime, the following inequality could be derived, based on Lemma 3.2:

$$\frac{1}{\Delta t} |((\mathcal{L}_{\check{\mathcal{M}}^n}(\rho^* - \rho^n))_{i_0,j_0,k_0} - (\mathcal{L}_{\check{\mathcal{M}}^n}(\rho^* - \rho^n))_{i_1,j_1,k_1})| \leq 2\tilde{C}_2\mathcal{M}_0^{-1}h^{-1/2}\Delta t^{-1}.$$

Since  $G_a^1(x)$  is an increasing function in terms of  $x > 0$  for any fixed  $a > 0$ , and  $\rho^n$  satisfies the bound (3.51), it is straightforward to obtain

$$\begin{aligned} &(G_{\rho^n}^1(\rho^*))_{i_0,j_0,k_0} - (G_{\rho^n}^1(\rho^*))_{i_1,j_1,k_1} + \langle C_n, \delta\psi \rangle \\ &\leq \ln M_h + 1 - G_{\epsilon_0}^1(\beta_0) + \Delta t(\ln M_h - \ln \epsilon_0). \end{aligned}$$

As a consequence, a combination of the above estimates leads to

$$(3.54) \quad \frac{1}{h^3} \frac{J_n(\rho^* + s\delta\psi) - J_n(\rho^*)}{s} \Big|_{s=0} \leq D_0 + \Delta t(\ln \delta - \ln \beta_0),$$

where  $D_0 = 2\tilde{C}_2\mathcal{M}_0^{-1}h^{-1/2}\Delta t^{-1} + \ln M_h + 1 - G_{\epsilon_0}^1(\beta_0) + \Delta t(\ln M_h - \ln \epsilon_0)$ , a constant for fixed  $\Delta t$  and  $h$ . Hence, we can choose  $\delta$  sufficiently small such that

$$(3.55) \quad \frac{1}{h^3} \frac{J_n(\rho^* + s\delta\psi) - J_n(\rho^*)}{s} \Big|_{s=0} < 0.$$

This inequality contradicts the assumption that  $\rho^*$  is a minimizer of  $J_n(\rho)$ . Therefore, a minimizer of  $J_n(\rho)$  cannot occur on the boundary of  $V_{h,\delta}^H$  if  $\delta$  is small enough. In other words, the minimizer of  $J_n(\rho)$  over  $V_h^H$  could only possibly occur at its interior point, which gives a solution of the numerical scheme (3.41). The uniqueness of this numerical solution comes from a direct application of the strict convexity of  $J_n(\rho)$ . The proof of Theorem 3.5 is complete.  $\square$

*Remark 3.3.* In both Theorem 3.1 and Theorem 3.5, the positivity-preserving property is established by using the singular nature of the logarithmic function. It is worth mentioning that the positivity-preserving property could also be proved by other classical methods, such as the method of upper and lower solutions [55].

With the positivity-preserving property and the unique solvability established, we can further prove the following unconditional energy stability.

**THEOREM 3.6.** *For the numerical solution (3.41), we have*

$$(3.56) \quad \mathcal{F}_h(\rho^{n+1}) \leq \mathcal{F}_h(\rho^n), \quad \text{with } \mathcal{F}_h(\rho^n) = \langle \rho^n \ln \rho^n + C\rho^n, \mathbf{1} \rangle.$$

*Proof.* Taking a discrete inner product with (3.41) by  $\mu^{n+1/2}$  yields

$$(3.57) \quad \frac{1}{\Delta t} \langle \rho^{n+1} - \rho^n, \mu^{n+1/2} \rangle = -\langle \mathcal{M}_h^{n+1/2} \nabla_h \mu^{n+1/2}, \nabla_h \mu^{n+1/2} \rangle \leq 0.$$

Note that

$$(3.58) \quad \begin{aligned} \langle \rho^{n+1} - \rho^n, \mu^{n+1/2} \rangle &= \mathcal{F}_h(\rho^{n+1}) - \mathcal{F}_h(\rho^n) + \Delta t \langle \rho^{n+1} - \rho^n, \ln \rho^{n+1} - \ln \rho^n \rangle \\ &\geq \mathcal{F}_h(\rho^{n+1}) - \mathcal{F}_h(\rho^n), \end{aligned}$$

due to the monotonic property of the logarithmic function. Then we arrive at

$$(3.59) \quad \mathcal{F}_h(\rho^{n+1}) - \mathcal{F}_h(\rho^n) \leq -\langle \mathcal{M}_h^{n+1/2} \nabla_h \mu^{n+1/2}, \nabla_h \mu^{n+1/2} \rangle \leq 0. \quad \square$$

*Remark 3.4.* It is worth emphasizing that the discretization presented in (3.41) is based on the  $H^{-1}$ -gradient flow structure of the diffusion equations. One can also construct a variational structure-preserving scheme for diffusion equations by using the Lagrangian methods [8, 38, 48], which treat diffusion equations as an  $L^2$ -gradient flow in the space of diffeomorphism, or the numerical methods for Wasserstein gradient flows in the space of probability measure [3].

**3.3. The second-order accurate operator splitting scheme.** The second-order operator splitting scheme could be formulated as follows, based on the previous analyses.

Given  $\mathbf{c}^n$  with  $\mathbf{c}_{i,j,k}^n \in \mathbb{R}_+^N$ , we update  $\mathbf{c}^{n+1}$  via the following three stages.

**Stage 1.** We set  $\mathbf{c}_0 = \mathbf{c}^n$  and solve the reaction trajectory equation, subject to the initial condition  $R^n = 0$ , using scheme (3.11) with a temporal step-size  $\Delta t/2$ . An intermediate numerical profile is updated as

$$(3.60) \quad \mathbf{c}^{n+1,(1)} = \mathbf{c}^n + \boldsymbol{\sigma} R^{n+1,(1)}.$$

**Stage 2.** Starting with the intermediate variable  $\mathbf{c}^{n+1,(1)}$ , we solve the diffusion equation  $\partial_t \mathbf{c} = \mathcal{B} \mathbf{c}$  by applying either scheme (3.36) (for constant diffusion coefficient) or scheme (3.41) (for nonlinear diffusion coefficient), with a temporal step-size  $\Delta t$ , to obtain  $\mathbf{c}^{n+1,(2)}$ .

**Stage 3.** We set  $\mathbf{c}_0 = \mathbf{c}^{n+1,(2)}$  and repeat the numerical algorithm at Stage 1, i.e., solving the reaction trajectory equation, subject to the initial condition  $R^n = 0$ , by scheme (3.11) with the temporal step-size  $\Delta t/2$  to obtain  $R^{n+1,(2)}$ . The numerical solution at  $t^{n+1}$  is updated as

$$(3.61) \quad \mathbf{c}^{n+1} = \mathbf{c}^{n+1,(2)} + \sigma R^{n+1,(2)}.$$

The following theoretical result for the second-order operator splitting scheme can be established, based on Theorems 3.1–3.6.

**THEOREM 3.7.** *Given  $\mathbf{c}^n$  with  $\mathbf{c}_{i,j,k}^n \in \mathbb{R}_+^N \forall 0 \leq i, j, k \leq N_0 - 1$  and the discrete periodic boundary condition, there exists a unique solution  $\mathbf{c}^{n+1}$  with  $\mathbf{c}_{i,j,k}^{n+1} \in \mathbb{R}_+^N \forall 0 \leq i, j, k \leq N_0 - 1$  for the second-order accurate operator splitting numerical scheme. In addition, we have the energy dissipation estimate*

$$\mathcal{F}_h(\mathbf{c}^{n+1}) \leq \mathcal{F}_h(\mathbf{c}^n),$$

so that  $\mathcal{F}_h(\mathbf{c}^n) \leq \mathcal{F}_h(\mathbf{c}^0)$ , which is a constant independent of  $h$ .

**4. The numerical results.** In this section, we present some numerical results to demonstrate the performance of the proposed numerical schemes.

**4.1. Reaction kinetics.** We first test the accuracy for the algorithm (3.11) by considering a simple reaction kinetics (with  $\alpha > 0$ ),

$$(4.1) \quad \begin{cases} \frac{dc_1}{dt} = c_2 - \alpha c_1, \\ \frac{dc_2}{dt} = \alpha c_1 - c_2, \end{cases}$$

which describes a simple reversible chemical reaction  $X_1 \xrightleftharpoons[1]{a} X_2$ . For any given initial value  $c_i(0) = c_i^0$ , the exact solution is given by

$$(4.2) \quad c_1(t) = \left(1 + \left(\frac{c_1^0}{c_1^\infty} - 1\right) \exp(-(a+1)t)\right) c_1^\infty, \quad c_2(t) = c_1^0 + c_2^0 - c_1(t),$$

with  $c_1^\infty = (c_1^0 + c_2^0)/(\alpha + 1)$  being the equilibrium concentration of  $X_1$ . Following the earlier analysis, we introduce  $R$  as the reaction trajectory, so that the energy-dissipation law of the system becomes

$$(4.3) \quad \frac{d}{dt} \left( \sum_{i=1}^2 c_i (\ln c_i - 1) + c_1 \ln a + c_2 \ln(1) \right) = -\dot{R} \ln \left( \frac{\dot{R}}{c_2} + 1 \right).$$

To test the order of the numerical accuracy, we display the errors between the numerical solution and exact solution at  $T = 1$  in Table 4.1, with a sequence of step-sizes  $\Delta t$ . An almost perfect second-order temporal accuracy is observed.

**4.2. A reaction-diffusion system.** In this subsection, we consider the reaction-diffusion system

$$(4.4) \quad \begin{cases} \partial_t u = D_u \Delta u^\alpha - k_1^+ uv^2 + k_1^- v^3, \\ \partial_t v = D_v \Delta v + k_1^+ uv^2 - k_1^- v^3, \end{cases}$$

TABLE 4.1  
 Error table for the linear ODE system (4.1).

$\Delta t$	Error	Order
1/20	2.0882e-3	
1/40	5.3413e-4	1.9670
1/80	1.3577e-4	1.9760
1/160	3.4279e-5	1.9858
1/320	8.6159e-6	1.9923
1/640	2.1600e-06	1.9960

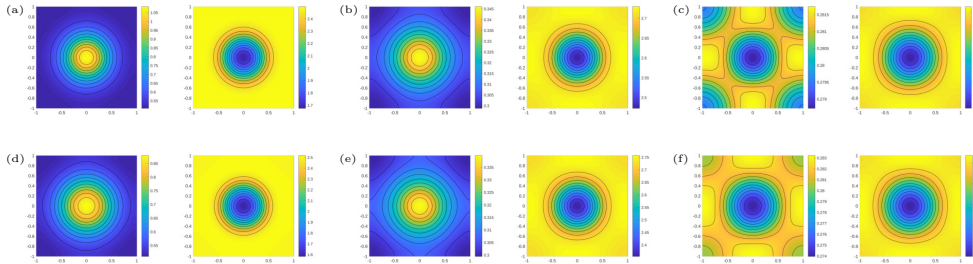
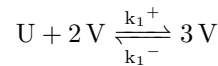


FIG. 4.1. Numerical solutions for the reaction-diffusion system (4.4) with  $\alpha = 1$  (a)–(c) and  $\alpha = 2$  (d)–(f) at  $t = 0.2$  (a) and (d),  $t = 0.5$  (b) and (e), and  $t = 0.7$  (c) and (f).

where  $\alpha \geq 1$  is a constant, and  $D_u > 0$  and  $D_v > 0$  are diffusion coefficients. The reaction part of (4.4) describes the chemical reaction



with the LMA. The whole system satisfies the energy-dissipation law

$$\begin{aligned} & \frac{d}{dt} \int_{\Omega} u(\ln u - 1 + U_u) + v(\ln v - 1 + U_v) d\mathbf{x} \\ & = - \int_{\Omega} \dot{R} \ln \left( \frac{\dot{R}}{k_1^- v^3} + 1 \right) + \alpha u^\alpha D_u |\nabla \mu_u|^2 + D_v |\nabla \mu_v|^2 d\mathbf{x}. \end{aligned}$$

The internal energies can be taken as  $U_u = \ln k_1^+$  and  $U_v = \ln k_1^-$  so that  $\dot{R} = k_1^+ uv^2 - k_1^- v^3$ .

For  $\alpha = 1$ , we apply the ETD scheme (3.36) to solve the diffusion parts for both  $u$  and  $v$ . Otherwise, we use scheme (3.41) for  $u$  and use the ETD scheme for  $v$ . The computational domain is taken as  $\Omega = (-1, 1)^2$ , and a periodic boundary condition is imposed for both  $u$  and  $v$ . The initial value is set as

$$\begin{aligned} u &= (-\tanh((\sqrt{x^2 + y^2} - 0.4)/0.1) + 1)/2 + 1; \\ v &= (\tanh((\sqrt{x^2 + y^2} - 0.4)/0.1) + 1)/2 + 1. \end{aligned}$$

Other parameters are taken as  $D_u = 0.2$ ,  $D_v = 0.1$ ,  $k_1^+ = 1$ , and  $k_1^- = 0.1$ .

Figure 4.1 shows the numerical solutions at  $t = 0.2, 0.5$ , and  $0.7$  for  $\alpha = 1$  and  $\alpha = 2$ , respectively, which are obtained by taking  $h = \Delta t = 1/20$ . The discrete

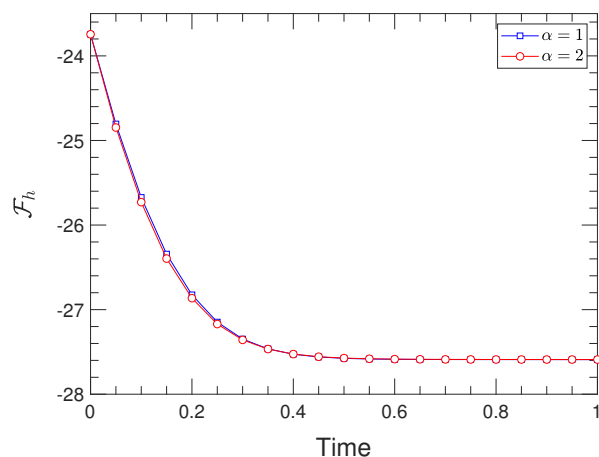


FIG. 4.2. The discrete free energy evolutions corresponding to numerical solutions for the reaction-diffusion system (4.4) with  $\alpha = 1$  and  $\alpha = 2$  ( $h = \Delta t = 1/20$ ).

free energy evolutions corresponding to these two numerical solutions are displayed in Figure 4.2, which clearly demonstrates the energy stability of the operator splitting scheme in both linear and nonlinear diffusion cases.

Next, we test for numerical accuracy of the operator splitting scheme. As analytical forms of the exact solutions are not available, we perform a Cauchy convergence test for numerical simulations for  $\alpha = 1$  and  $\alpha = 2$ , respectively, at  $T = 0.2$ , before the systems reach their constant equilibria. We compute the  $\ell^\infty$  differences between numerical solutions with consecutive spatial resolutions  $h_{j-1}$ ,  $h_j$ , and  $h_{j+1}$ , with  $\Delta t_j = h_j$ . Since we expect the numerical scheme to preserve a second-order spatial accuracy, we could compute the quantity

$$\frac{\ln\left(\frac{1}{A^*} \cdot \frac{\|u_{h_{j-1}} - u_{h_j}\|_\infty}{\|u_{h_j} - u_{h_{j+1}}\|_\infty}\right)}{\ln \frac{h_{j-1}}{h_j}}, \quad A^* = \frac{1 - \frac{h_j^2}{h_{j-1}^2}}{1 - \frac{h_{j+1}^2}{h_j^2}}, \quad \text{for } h_{j-1} > h_j > h_{j+1},$$

to check the convergence order [47]. As demonstrated in Tables 4.2 and 4.3, an almost perfect second-order accuracy has been achieved for both the linear and nonlinear diffusion cases.

**4.3. Reversible Gray–Scott model.** The Gray–Scott model is one of the most famous reaction-diffusion models, due to the complex pattern formulation phenomenon [32, 56]. The classical Gray–Scott system is given by

$$(4.5) \quad \begin{cases} u_t = D_u \Delta u - k_1^+ uv^2 + \alpha(1 - u), \\ v_t = D_v \Delta v + k_1^+ uv^2 - k_2^+ v, \end{cases}$$

which corresponds to the two reactions



where  $P$  is the inert product. Additionally, there exists a birth-death process that feeds and drains  $U$  with the rate  $\alpha$  in the system. The chemical reactions in the

TABLE 4.2

The  $\ell^\infty$  differences and convergence order for the numerical solutions of  $u$  and  $v$  for (4.4) with  $\alpha = 1$ . Various mesh resolutions are used:  $h_1 = \frac{1}{20}$ ,  $h_2 = \frac{1}{30}$ ,  $h_3 = \frac{1}{40}$ ,  $h_4 = \frac{1}{50}$ ,  $h_5 = \frac{1}{60}$ , and the temporal step-size is taken as  $\Delta t_j = h_j$ .

—	$\psi = u$	Order	$\psi = v$	Order
$\ \psi_{h_1} - \psi_{h_2}\ _\infty$	4.1625e-3	-	3.6818e-3	-
$\ \psi_{h_2} - \psi_{h_3}\ _\infty$	1.5357e-3	1.8700	1.3581e-3	1.8705
$\ \psi_{h_3} - \psi_{h_4}\ _\infty$	7.3080e-4	1.9036	6.4788e-4	1.8950
$\ \psi_{h_4} - \psi_{h_5}\ _\infty$	4.0386e-4	1.9230	3.5830e-4	1.9197

TABLE 4.3

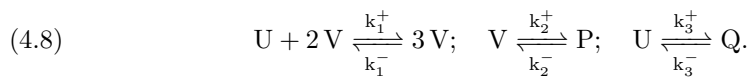
The  $\ell^\infty$  differences and convergence order for the numerical solutions of  $u$  and  $v$  for (4.4) with  $\alpha = 2$  at  $T = 0.2$ . Various mesh resolutions are used:  $h_1 = \frac{1}{20}$ ,  $h_2 = \frac{1}{30}$ ,  $h_3 = \frac{1}{40}$ ,  $h_4 = \frac{1}{50}$ ,  $h_5 = \frac{1}{60}$ , and the temporal step-size is taken as  $\Delta t_j = h_j$ .

—	$\psi = u$	Order	$\psi = v$	Order
$\ \psi_{h_1} - \psi_{h_2}\ _\infty$	4.4205e-3	-	2.6961e-3	-
$\ \psi_{h_2} - \psi_{h_3}\ _\infty$	1.4508e-3	2.1586	9.4864e-4	1.9870
$\ \psi_{h_3} - \psi_{h_4}\ _\infty$	6.1387e-4	2.3120	4.3720e-4	2.0150
$\ \psi_{h_4} - \psi_{h_5}\ _\infty$	3.1575e-4	2.2446	2.4420e-4	1.8752

classical Gray–Scott model are not reversible. However, one can view the irreversible Gray–Scott as a certain limit of a reversible Gray–Scott system, given by [43]

$$(4.7) \quad \begin{cases} \partial_t u = D_u \Delta u - k_1^+ u v^2 + k_1^- v^3 - k_3^+ u + k_3^- q, \\ \partial_t v = D_v \Delta v + k_1^- u v^2 - k_1^- v^3 - k_2^+ v + k_2^- p, \\ \partial_t p = D_p \Delta p + k_2^+ v - k_2^- q, \\ \partial_t q = D_q \Delta q + k_3^+ u - k_3^- q, \end{cases}$$

in which the reversible chemical reactions are given by



Formally, the reversible system converges to the classical Gray–Scott system if  $k_1^- \rightarrow 0$ ,  $k_2^- \rightarrow 0$ ,  $k_3^+ = \alpha$ , and  $k_3^- q \rightarrow \alpha$ . In this subsection, we perform a numerical simulation of the reversible Gray–Scott model (4.7), which can be derived from the energy-dissipation law

$$(4.9) \quad \begin{aligned} & \frac{d}{dt} \int u(\ln u - 1) + uU_u + v(\ln v - 1) + vU_v + p(\ln p - 1) + pU_p + q(\ln q - 1) + qU_q \\ &= - \int \frac{1}{D_u} u |\mathbf{u}_u|^2 + \frac{1}{D_v} v |\mathbf{u}_v|^2 + \frac{1}{D_p} p |\mathbf{u}_p|^2 + \frac{1}{D_q} q |\mathbf{u}_q|^2 \\ & \quad + \dot{R}_1 \ln \left( \frac{\dot{R}_1}{k_1^- v^3} + 1 \right) + \dot{R}_2 \ln \left( \frac{\dot{R}_2}{k_2^- p} + 1 \right) + \dot{R}_3 \ln \left( \frac{\dot{R}_3}{k_3^- q} + 1 \right) d\mathbf{x}, \end{aligned}$$

where  $U_u, U_v, U_p$ , and  $U_q$  are internal energies that determine the reaction rates. One can take

$$(4.10) \quad \begin{aligned} U_u &= \ln k_3^+, \quad U_v = \ln k_3^+ + \ln k_1^- - \ln k_1^+, \\ U_p &= \ln k_3^+ + \ln k_1^- + \ln k_2^- - \ln k_1^+ - \ln k_2^+, \quad U_q = \ln k_3^-. \end{aligned}$$

In the numerical simulation, we set the computational domain as  $(0, 2.5)^2$  and take

$$k_1^+ = 1, \quad k_2^+ = 0.084, \quad k_1^- = k_2^- = 10^{-6}, \quad k_3^+ = 0.024, \quad k_3^- = 10^{-2},$$

$$D_u = 8 \times 10^{-4}, \quad D_v = 4 \times 10^{-4}, \quad D_p = D_q = 10.$$

The initial conditions are

$$(4.11) \quad v(x, y, 0) = \begin{cases} \frac{1}{4} \sin^2(4\pi x) \sin^2(4\pi y) + 0.1, & 1 \leq x, y \leq 1.5, \\ 0.1 & \text{otherwise,} \end{cases}$$

$$u(x, y, 0) = 1 - 2v(x, y, 0), \quad p(x, y, 0) = 1, \quad q(x, y, 0) = 2.4.$$

The nonflux boundary condition is imposed for all variables. The numerical example is modified from a numerical example in [34]. The initial condition of  $q$  is chosen such that  $k_3^- q(x, y, 0) = k_3^+$ . Figure 4.3(a)–(f) shows the time evolution of the  $v$ -component at various times with  $\Delta t = 0.1$  and  $h = 1/50$ . The solutions are only displayed in  $0.5 \leq x, y \leq 2$  for visualization. The evolution of the discrete free energy is shown in Figure 4.3(g).

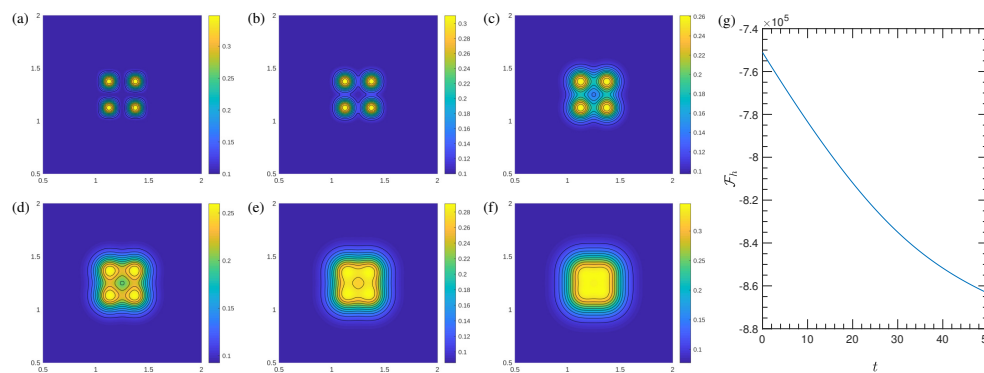


FIG. 4.3. Time evolution of  $v$  in the reversible Gray–Scott model at various times: (a)  $t = 0$ , (b)  $t = 1$ , (c)  $t = 5$ , (d)  $t = 10$ , (e)  $t = 15$ , (f)  $t = 20$ . The solutions are only displayed in  $0.5 \leq x, y \leq 2$  for visualization. (g) Evolution of the discrete free energy with respect to time.

One can see that the proposed numerical scheme works well for a system with multiple chemical reactions. Unfortunately, under the current initial conditions and parameters, we didn't observe the pattern formulation as in [34]. It is still unclear whether the reversible Gray–Scott model can capture the pattern formation in the classical Gray–Scott model. A detailed numerical study will be carried out in future work.

**5. Concluding remarks.** A second-order accurate, operator splitting numerical scheme is developed for reaction-diffusion equations with the detailed balance condition based on their variational structures. The key idea is to design an operator splitting scheme such that each stage dissipates the same free energy, according to the variational structure associated with the original system. In the reaction part, the reaction trajectory equation is solved by using the numerical techniques from  $L^2$ -gradient flows, based on a modified Crank–Nicolson approach. In the diffusion part, an ETD algorithm gives an exact time integration for a linear diffusion, while a semi-implicit algorithm is applied for a nonlinear diffusion. A combination of the numerical

algorithms at both stages by the Strang splitting approach leads to the proposed operator splitting scheme. Moreover, the unique solvability and the positivity-preserving property, as well as an unconditional energy stability, can be proved for each stage; as a result, the combined splitting scheme also satisfies these theoretical properties. Similar ideas can be applied to other dissipative systems with multiple dissipation mechanisms. A few numerical results have also been presented to demonstrate the numerical performance.

**Acknowledgment.** Y. Wang would like to thank the Department of Applied Mathematics at Illinois Institute of Technology for their generous support and stimulating environment.

## REFERENCES

- [1] A. BASKARAN, Z. HU, J. LOWENGRUB, C. WANG, S. WISE, AND P. ZHOU, *Energy stable and efficient finite-difference nonlinear multigrid schemes for the modified phase field crystal equation*, J. Comput. Phys., 250 (2013), pp. 270–292.
- [2] A. BASKARAN, J. S. LOWENGRUB, C. WANG, AND S. M. WISE, *Convergence analysis of a second order convex splitting scheme for the modified phase field crystal equation*, SIAM J. Numer. Anal., 51 (2013), pp. 2851–2873, <https://doi.org/10.1137/120880677>.
- [3] J.-D. BENAMOU, G. CARLIER, AND M. LABORDE, *An augmented Lagrangian approach to Wasserstein gradient flows: From theory to application*, ESAIM Proc. Surveys, 54 (2016), pp. 1–17.
- [4] V. BERDICHEVSKY, *Variational Principles of Continuum Mechanics I: Fundamentals*, Springer-Verlag, 2009.
- [5] A. N. BERIS AND B. J. EDWARDS, *Thermodynamics of Flowing Systems with Internal Microstructure*, Oxford Engrg. Sci. Ser. 36, Oxford University Press, 1994.
- [6] E. BERTOLAZZI, *Positive and conservative schemes for mass action kinetics*, Comput. Math. Appl., 32 (1996), pp. 29–43.
- [7] M. A. BIOT, *Thermodynamic principle of virtual dissipation and the dynamics of physical-chemical fluid mixtures including radiation pressure*, Quart. Appl. Math., 39 (1982), pp. 517–540.
- [8] J. A. CARRILLO, B. DÜRING, D. MATTHES, AND D. S. MCCORMICK, *A Lagrangian scheme for the solution of nonlinear diffusion equations using moving simplex meshes*, J. Sci. Comput., 75 (2018), pp. 1463–1499.
- [9] J. A. CARRILLO, S. FAGIOLI, F. SANTAMBROGIO, AND M. SCHMIDTCHEN, *Splitting schemes and segregation in reaction cross-diffusion systems*, SIAM J. Math. Anal., 50 (2018), pp. 5695–5718, <https://doi.org/10.1137/17M1158379>.
- [10] W. CHEN, C. WANG, X. WANG, AND S. M. WISE, *Positivity-preserving, energy stable numerical schemes for the Cahn-Hilliard equation with logarithmic potential*, J. Comput. Phys. X, 3 (2019), 100031.
- [11] M. CHIPOT, D. KINDERLEHRER, AND M. KOWALCZYK, *A variational principle for molecular motors*, Meccanica, 38 (2003), pp. 505–518.
- [12] S. M. COX AND P. C. MATTHEWS, *Exponential time differencing for stiff systems*, J. Comput. Phys., 176 (2002), pp. 430–455.
- [13] T. DE DONDER, *L'affinité*, Mémoires de la Classe des Sciences, Vol. 9, Académie royale de Belgique: Collection in-8°, Gauthier-Villars, 1927.
- [14] T. DE DONDER, *Thermodynamic Theory of Affinity*, Vol. 1, Stanford University Press, 1936.
- [15] S. R. DE GROOT AND P. MAZUR, *Non-equilibrium Thermodynamics*, Courier Corporation, 1984.
- [16] S. DESCOMBES, *Convergence of a splitting method of high order for reaction-diffusion systems*, Math. Comp., 70 (2001), pp. 1481–1501.
- [17] A. DIEGEL, C. WANG, AND S. WISE, *Stability and convergence of a second order mixed finite element method for the Cahn-Hilliard equation*, IMA J. Numer. Anal., 36 (2016), pp. 1867–1897.
- [18] L. DONG, C. WANG, S. WISE, AND Z. ZHANG, *A positivity-preserving, energy stable scheme for a ternary Cahn-Hilliard system with the singular interfacial parameters*, J. Comput. Phys., 442 (2021), 110451.
- [19] L. DONG, C. WANG, H. ZHANG, AND Z. ZHANG, *A positivity-preserving, energy stable and convergent numerical scheme for the Cahn-Hilliard equation with a Flory-Huggins-deGennes*

- energy*, Commun. Math. Sci., 17 (2019), pp. 921–939.
- [20] L. DONG, C. WANG, H. ZHANG, AND Z. ZHANG, *A positivity-preserving second-order BDF scheme for the Cahn–Hilliard equation with variable interfacial parameters*, Commun. Comput. Phys., 28 (2020), pp. 967–998.
- [21] Q. DU, L. JU, X. LI, AND Z. QIAO, *Maximum principle preserving exponential time differencing schemes for the nonlocal Allen–Cahn equation*, SIAM J. Numer. Anal., 57 (2019), pp. 875–898, <https://doi.org/10.1137/18M118236X>.
- [22] Q. DU, L. JU, X. LI, AND Z. QIAO, *Maximum Bound Principles for a Class of Semilinear Parabolic Equations and Exponential Time Differencing Schemes*, preprint, <https://arxiv.org/abs/2005.11465>, 2020.
- [23] Q. DU AND R. A. NICOLAIDES, *Numerical analysis of a continuum model of phase transition*, SIAM J. Numer. Anal., 28 (1991), pp. 1310–1322, <https://doi.org/10.1137/0728069>.
- [24] R. EISENBERG, Y. HYON, AND C. LIU, *Energy variational analysis of ions in water and channels: Field theory for primitive models of complex ionic fluids*, J. Chem. Phys., 133 (2010), 104104.
- [25] L. FORMAGGIA AND A. SCOTTI, *Positivity and conservation properties of some integration schemes for mass action kinetics*, SIAM J. Numer. Anal., 49 (2011), pp. 1267–1288, <https://doi.org/10.1137/100789592>.
- [26] Z. FU AND J. YANG, *Energy-decreasing exponential time differencing Runge–Kutta methods for phase-field models*, J. Comput. Phys., 454 (2022), 110943.
- [27] D. FURIHATA AND T. MATSUO, *Discrete Variational Derivative Method: A Structure-Preserving Numerical Method for Partial Differential Equations*, CRC Press, 2010.
- [28] T. GALLOUËT, M. LABORDE, AND L. MONSAINGEON, *An unbalanced optimal transport splitting scheme for general advection–reaction–diffusion problems*, ESAIM Control Optim. Calc. Var., 25 (2019), 8.
- [29] T. O. GALLOUËT AND L. MONSAINGEON, *A JKO splitting scheme for Kantorovich–Fisher–Rao gradient flows*, SIAM J. Math. Anal., 49 (2017), pp. 1100–1130, <https://doi.org/10.1137/16M106666X>.
- [30] M.-H. GIGA, A. KIRSSTEIN, AND C. LIU, *Variational modeling and complex fluids*, in Handbook of Mathematical Analysis in Mechanics of Viscous Fluids, Springer, 2017, pp. 1–41.
- [31] J. GUO, C. WANG, S. WISE, AND X. YUE, *An  $H^2$  convergence of a second-order convex-splitting, finite difference scheme for the three-dimensional Cahn–Hilliard equation*, Commun. Math. Sci., 14 (2016), pp. 489–515.
- [32] W. HAO AND C. XUE, *Spatial pattern formation in reaction–diffusion models: A computational approach*, J. Math. Biol., 80 (2020), pp. 521–543.
- [33] A. HAWKINS-DAARUD, K. G. VAN DER ZEE, AND J. TINSLEY ODEN, *Numerical simulation of a thermodynamically consistent four-species tumor growth model*, Int. J. Numer. Methods Biomed. Eng., 28 (2012), pp. 3–24.
- [34] G. HU, Z. QIAO, AND T. TANG, *Moving finite element simulations for reaction–diffusion systems*, Adv. Appl. Math. Mech., 4 (2012), pp. 365–381.
- [35] Z. HU, S. WISE, C. WANG, AND J. LOWENGRUB, *Stable and efficient finite-difference nonlinear-multigrid schemes for the phase-field crystal equation*, J. Comput. Phys., 228 (2009), pp. 5323–5339.
- [36] J. HUANG AND C.-W. SHU, *Positivity-preserving time discretizations for production–destruction equations with applications to non-equilibrium flows*, J. Sci. Comput., 78 (2019), pp. 1811–1839.
- [37] F. JÜLICHER, A. AJDARI, AND J. PROST, *Modeling molecular motors*, Rev. Mod. Phys., 69 (1997), 1269–1282.
- [38] O. JUNGE, D. MATTHES, AND H. OSBERGER, *A fully discrete variational scheme for solving nonlinear Fokker–Planck equations in multiple space dimensions*, SIAM J. Numer. Anal., 55 (2017), pp. 419–443, <https://doi.org/10.1137/16M1056560>.
- [39] A.-K. KASSAM AND L. N. TREFETHEN, *Fourth-order time-stepping for stiff PDEs*, SIAM J. Sci. Comput., 26 (2005), pp. 1214–1233, <https://doi.org/10.1137/S1064827502410633>.
- [40] D. KONDEPUDI AND I. PRIGOGINE, *Modern Thermodynamics: From Heat Engines to Dissipative Structures*, John Wiley & Sons, 2014.
- [41] S. KONDO AND T. MIURA, *Reaction–diffusion model as a framework for understanding biological pattern formation*, Science, 329 (2010), pp. 1616–1620.
- [42] W. LI, W. CHEN, C. WANG, Y. YAN, AND R. HE, *A second order energy stable linear scheme for a thin film model without slope selection*, J. Sci. Comput., 76 (2018), pp. 1905–1937.
- [43] J. LIANG, N. JIANG, C. LIU, Y. WANG, AND T.-F. ZHANG, *On a reversible Gray–Scott type system from energetic variational approach and its irreversible limit*, J. Differential Equations, 309 (2022), pp. 427–454.

- [44] C. LIU, *An introduction of elastic complex fluids: An energetic variational approach*, in *Multi-Scale Phenomena in Complex Fluids: Modeling, Analysis and Numerical Simulation*, World Scientific, 2009, pp. 286–337.
- [45] C. LIU, C. WANG, AND Y. WANG, *A structure-preserving, operator splitting scheme for reaction-diffusion equations with detailed balance*, *J. Comput. Phys.*, 436 (2021), 110253, <https://doi.org/10.1016/j.jcp.2021.110253>.
- [46] C. LIU, C. WANG, Y. WANG, AND S. M. WISE, *Convergence analysis of the variational operator splitting scheme for a reaction-diffusion system with detailed balance*, *SIAM J. Numer. Anal.*, 60 (2022), pp. 781–803, <https://doi.org/10.1137/21M1421283>.
- [47] C. LIU, C. WANG, S. M. WISE, X. YUE, AND S. ZHOU, *A positivity-preserving, energy stable and convergent numerical scheme for the Poisson-Nernst-Planck system*, *Math. Comp.*, 90 (2021), pp. 2071–2106.
- [48] C. LIU AND Y. WANG, *On Lagrangian schemes for porous medium type generalized diffusion equations: A discrete energetic variational approach*, *J. Comput. Phys.*, 417 (2020), 109566.
- [49] C. LIU AND Y. WANG, *A Variational Lagrangian Scheme for a Phase Field Model: A Discrete Energetic Variational Approach*, preprint, <https://arxiv.org/abs/2003.10413>, 2020.
- [50] J.-G. LIU, M. TANG, L. WANG, AND Z. ZHOU, *An accurate front capturing scheme for tumor growth models with a free boundary limit*, *J. Comput. Phys.*, 364 (2018), pp. 73–94.
- [51] A. MIELKE, R. I. A. PATTERSON, M. A. PELETIER, AND D. R. MICHIEL RENGER, *Non-equilibrium thermodynamical principles for chemical reactions with mass-action kinetics*, *SIAM J. Appl. Math.*, 77 (2017), pp. 1562–1585, <https://doi.org/10.1137/16M1102240>.
- [52] L. ONSAGER, *Reciprocal relations in irreversible processes I*, *Phys. Rev.*, 37 (1931), pp. 405–426.
- [53] L. ONSAGER, *Reciprocal relations in irreversible processes II*, *Phys. Rev.*, 38 (1931), pp. 2265–2279.
- [54] G. F. OSTER AND A. S. PERELSON, *Chemical reaction dynamics*, *Arch. Rational Mech. Anal.*, 55 (1974), pp. 230–274.
- [55] C. V. PAO, *Nonlinear Parabolic and Elliptic Equations*, Springer, 2012.
- [56] J. E. PEARSON, *Complex patterns in a simple system*, *Science*, 261 (1993), pp. 189–192.
- [57] B. PERTHAME, F. QUIRÓS, AND J. L. VÁZQUEZ, *The Hele–Shaw asymptotics for mechanical models of tumor growth*, *Arch. Ration. Mech. Anal.*, 212 (2014), pp. 93–127.
- [58] J. PROST, F. JÜLICHER, AND J.-F. JOANNY, *Active gel physics*, *Nat. Phys.*, 11 (2015), pp. 111–117.
- [59] Y. QIAN, C. WANG, AND S. ZHOU, *A positive and energy stable numerical scheme for the Poisson-Nernst-Planck-Cahn-Hilliard equations with steric interactions*, *J. Comput. Phys.*, 426 (2021), 109908.
- [60] L. RAYLEIGH, *Note on the numerical calculation of the roots of fluctuating functions*, *Proc. London Math. Soc.*, 1 (1873), pp. 119–124.
- [61] J. SHEN, C. WANG, X. WANG, AND S. M. WISE, *Second-order convex splitting schemes for gradient flows with Ehrlich–Schwoebel type energy: Application to thin film epitaxy*, *SIAM J. Numer. Anal.*, 50 (2012), pp. 105–125, <https://doi.org/10.1137/110822839>.
- [62] G. STRANG, *On the construction and comparison of difference schemes*, *SIAM J. Numer. Anal.*, 5 (1968), pp. 506–517, <https://doi.org/10.1137/0705041>.
- [63] H. WANG, C. S. PESKIN, AND T. C. ELSTON, *A robust numerical algorithm for studying biomolecular transport processes*, *J. Theoret. Biol.*, 221 (2003), pp. 491–511.
- [64] Y. WANG, C. LIU, P. LIU, AND B. EISENBERG, *Field theory of reaction-diffusion: Law of mass action with an energetic variational approach*, *Phys. Rev. E*, 102 (2020), 062147.
- [65] Y. WANG, T.-F. ZHANG, AND C. LIU, *A Two Species Micro-Macro Model of Wormlike Micellar Solutions and Its Maximum Entropy Closure Approximations: An Energetic Variational Approach*, preprint, <https://arxiv.org/abs/2101.09838>, 2021.
- [66] Y. YAN, W. CHEN, C. WANG, AND S. WISE, *A second-order energy stable BDF numerical scheme for the Cahn-Hilliard equation*, *Commun. Comput. Phys.*, 23 (2018), pp. 572–602.
- [67] S. ZHAO, J. OVADIA, X. LIU, Y.-T. ZHANG, AND Q. NIE, *Operator splitting implicit integration factor methods for stiff reaction-diffusion-advection systems*, *J. Comput. Phys.*, 230 (2011), pp. 5996–6009.